Septate junction proteins are required for egg elongation and border cell migration during oogenesis in Drosophila

Haifa Alhadyian[1], Dania Shoiab[1], and Robert E. Ward IV[1,2]

[1]Department of Molecular Biosciences, University of Kansas, Lawrence, Kansas 66045

[2]Current address and Corresponding Author information: Robert E. Ward IV, Department of Biology, Case Western Reserve University, 2080 Adelbert Rd, Cleveland, Ohio 44106

E-mail: rew130@case.edu

Phone: (216) 368-6707

Running title: SJ proteins in oogenesis

Keywords: Septate junctions, oogenesis, Drosophila, tissue morphogenesis, egg elongation

Abstract

Protein components of the invertebrate occluding junction - known as the septate junction (SJ) - are required for morphogenetic developmental events during embryogenesis in *Drosophila melanogaster*. In order to determine whether SJ proteins are similarly required for morphogenesis during other developmental stages, we investigated the localization and requirement of four representative SJ proteins during oogenesis: Contactin, Macroglobulin complement-related, Neurexin IV, and Coracle. A number of morphogenetic processes occur during oogenesis, including egg elongation, formation of dorsal appendages, and border cell migration. We found that all four SJ proteins are expressed in the egg throughout oogenesis, with the highest and most sustained levels in the follicular epithelium (FE). In the FE, SJ proteins localize along the lateral membrane during early and mid-oogenesis, but become enriched in an apical-lateral domain (the presumptive SJ) by stage 10b. SJ protein relocalization requires the expression of other SJ proteins, as well as rab5 and rab11 in a manner similar to SJ biogenesis in the embryo. Knocking down the expression of these SJ proteins in follicle cells throughout oogenesis results in egg elongation defects and abnormal dorsal appendages. Similarly, reducing the expression of SJ genes in the border cell cluster results in border cell migration defects. Together, these results demonstrate an essential requirement for SJ genes in morphogenesis during oogenesis, and suggests that SJ proteins may have conserved functions in epithelial morphogenesis across developmental stages.

35 **Article Summary**

36 Septate junction (SJ) proteins are essential for forming an occluding junction in epithelial tissues
37 of *Drosophila melanogaster*. SJ proteins are also required for morphogenetic events during
38 embryogenesis prior to the formation of an occluding junction. To determine if SJ proteins
39 function in morphogenesis at other developmental stages, we examined their function during
40 oogenesis, and found that SJ proteins are expressed in the follicular epithelium of the egg
41 chamber and are required for egg elongation, dorsal appendages formation, and border cell
42 migration. Additionally, we found that the formation of SJs in oogenesis is similar to that in
43 embryonic epithelia.

44 **Introduction**

45 The septate junction (hereafter referred to as SJ) provides an essential paracellular barrier to
46 epithelial tissues in invertebrate animals (Noirot-timothée *et al.* 1978). As such, the SJ is
47 functionally equivalent to the tight junction in vertebrate tissues, although the molecular
48 components and ultrastructure of these junctions differ (reviewed in Izumi and Furuse 2014).
49 Studies in *Drosophila* have identified more than 20 proteins that are required for the organization
50 or maintenance of the SJ (Fehon *et al.* 1994; Baumgartner *et al.* 1996; Behr *et al.* 2003; Paul *et*
51 *al.* 2003; Genova and Fehon 2003; Faivre-Sarrailh *et al.* 2004; Wu *et al.* 2004; Wu *et al.* 2007;
52 Tiklová *et al.* 2010; Nelson *et al.* 2010; Ile *et al.* 2012; Bätz *et al.* 2014; Hall *et al.* 2014). Given
53 that some of these genes have clear developmental functions (e.g. *coracle*'s name derives from
54 its dorsal open embryonic phenotype; (Fehon *et al.* 1994), we previously undertook an
55 examination of the developmental requirements for a set of core SJ genes (Hall and Ward 2016).
56 We found that all of the genes we analyzed (9 in all) are required for morphogenetic
57 developmental events during embryogenesis including head involution, dorsal closure and
58 salivary gland organogenesis. Interestingly, these embryonic developmental events occur prior to
59 the formation of an intact SJ, suggesting that these proteins have a function independent of their
60 role in creating the occluding junction (Hall and Ward 2016). Since strong loss of function
61 mutations in every SJ gene are embryonic lethal (due to these morphogenetic defects and/or a
62 failure in establishing a blood-brain barrier in glial cells; Baumgartner *et al.* 1996), only a few
63 studies have examined the role of SJ proteins in morphogenesis at a later stages of development
64 (Lamb *et al.* 1998; Venema *et al.* 2004; Moyer and Jacobs 2008; Banerjee *et al.* 2008). These

65 studies have revealed roles for SJ proteins in planar polarization of the wing imaginal disc, for
66 epithelial rotations in the eye and genital imaginal discs, and ommatidia integrity.
67 To further explore the role of SJ proteins in morphogenesis beyond the embryonic stage, we
68 set out to examine the expression and function of a subset of SJ genes in the *Drosophila* egg
69 chamber during oogenesis. Each of the two *Drosophila* ovaries is comprised of approximately
70 16-20 ovarioles, which are organized into strings of progressively developing egg chambers
71 (Figure 1A). Each egg chamber forms in a structure called the germarium, where the germline
72 and somatic stem cells reside. Once the egg chamber is formed, it leaves the germarium as 16-
73 cell germline cyst consisting of 15 nurse cells and an oocyte surrounded by a layer of somatic
74 follicle cells (FCs) (Figure 1B). An egg chamber undergoes 14 developmental stages ending in a
75 mature egg that is ready for fertilization (reviewed in Horne-Badovinac and Bilder 2005).
76 Interfollicular cells called stalk cells connect egg chambers to each other. During oogenesis, the
77 follicular epithelium (FE) undergoes several morphogenetic events including border cell
78 migration, dorsal appendage formation and egg elongation (reviewed in Horne-Badovinac and
79 Bilder 2005; reviewed in Duhart *et al.* 2017).
80 Previous studies have revealed that a few core components of the SJ are expressed in the
81 ovary, including Macroglobulin complement-related (Mcr), Neurexin IV (Nrx-IV), Contactin
82 (Cont), Neuroglian (Nrg), and Coracle (Cora) (Wei *et al.* 2004; Schneider *et al.* 2006; Maimon *et*
83 *al.* 2014; Hall *et al.* 2014; Ben-Zvi and Volk 2019), although the developmental expression
84 pattern and subcellular localizations of these proteins have not been thoroughly investigated.
85 Furthermore, ultrastructural analysis has revealed the presence of mature SJs in the FE by stage
86 10/10b of oogenesis, while incipient SJ structures have been observed in egg chambers as early
87 as stage 6 (Mahowald 1972; Müller 2000). The biogenesis of SJs in embryonic epithelia is a

88 multistep process in which SJ proteins are initially localized along the lateral membrane, but
89 become restricted to an apical-lateral region (the SJ) in a process that required endocytosis and
90 recycling of SJ proteins (Tiklová *et al.* 2010). How SJ maturation occurs in the FE is unknown.
91 Here, we analyzed the expression and subcellular localization of the core SJ proteins Mcr,
92 Cont, Nrx-IV, and Cora throughout oogenesis. We find that all of these SJ proteins are expressed
93 in the FE throughout oogenesis. Interestingly, Mcr, Cont, Nrx-IV, and Cora become enriched at
94 the most apical-lateral region of the membrane in stage 10b/11 egg chambers, coincident with
95 the formation of the SJ revealed by electron microscopy (Mahowald 1972; Müller 2000) .
96 Similar to the biogenesis of SJs in the embryo, this enrichment of SJ proteins to the presumptive
97 SJ requires the function of other SJ genes, as well as *Rab5* and *Rab11*. Functional studies using
98 RNA interference (RNAi) of SJ genes in FCs results in defects in egg elongation, dorsal
99 appendage morphogenesis and border cell migration. Together, these results reveal a strong
100 similarity in the biogenesis of SJ between embryonic and follicular epithelia, and demonstrate
101 that at least some components of the SJs are required for morphogenesis in the ovary, and
102 suggest that these roles may be independent of their role in forming an occluding junction.
103
104

105 **Material and methods**

106 *Fly stocks*

107 All *Drosophila* stocks were maintained on media consisting of corn meal, sugar, yeast, and agar
108 in incubators maintained at a constant temperature of 25°. GAL4 lines used in this study are as
109 follows: *GR1-GAL4* (Bloomington Drosophila Stock Center (BDSC) #36287), *Slbo-GAL4, UAS-*
110 *mCD8-GFP* (BDSC#76363), and *C306-GAL4; GAL80^{ts}/Cyo* (a gift from Jocelyn McDonald,
111 Kansas State University, Manhattan, Kansas). RNAi stocks used for these studies are as follows:
112 *UAS-Mcr-RNAi* (BDSC#65896 and Vienna Drosophila Resources Center (VDRC)#100197),
113 *UAS-cora-RNAi* (BDSC#28933 and VDRC#9787), *UAS-Nrx-IV-RNAi* (BDSC#32424 and
114 VDRC#9039), *UAS-Cont-RNAi* (BDSC#28923), *UAS-mCherry-RNAi* (BDSC#35787), *UAS-Lac-*
115 *RNAi* (BDSC#28940), and *UAS-Sinu-RNAi* (VDRC#44929). *UAS-Rab5^{DN}* (BDSC#9771) was
116 used to inhibit normal Rab5 function and *UAS-Rab11-RNAi* (BDSC#27730) was used to knock
117 down Rab11 in the follicle cells. *UAS-GAL80^{ts}* (BDSC#7108) was used to deactivate GR1-GAL4
118 activity in Rab11-RNAi experiment. *UAS-GFP* (BDSC#1521) was crossed to *GR1-GAL4* as a
119 control for the egg shape experiments, whereas *Slbo-GAL4, UAS-mCD8-GFP* was crossed to
120 *UAS-mCherry-RNAi* as a control for border cell migration studies. Additionally, *C306-GAL4;*
121 *GAL80^{ts}/Cyo* was crossed to *UAS-Dcr* (BDSC#24646) as a control for border cell migration
122 studies. *w^{1118}* (BDSC# 5905) was used as the wild type stock for determining the expression of
123 Mcr, Cont, Nrx-IV and Cora in the follicle cells. *Rab5-YFP* (BDSC#62543) and *Rab11YFP*

124 (BDSC#62549) were used to determine their co-localization with Mcr in the follicle cells at stage
125 10.
126
127 *Fly staging*
128 w^{1118} 1-2-day-old females and males were collected and reared at 25ºC on fresh food sprinkled
129 with yeast for five to six days before the females were dissection for antibody staining. For egg
130 elongation analyses, crosses were maintained at 25ºC, and 1-2-day-old females (control and
131 *UAS-RNAi*-expressing) were mated with sibling males and maintained at 29-30ºC for 3 days
132 before dissection. For border cell migration analyses, *Slbo-GAL4* crosses were kept at 25ºC,
133 whereas *C306-GAL4/UAS-Dcr; GAL80^{ts}/SJ-RNAi* crosses were kept at 18ºC to prevent GAL4
134 activation. 1-2-day-old flies with the appropriate genotype (*Slbo-GAL4, UAS-mCD8-GFP/UAS-*
135 *RNAi* or *C306-GAL4 /UAS-Dcr;UAS-RNAi;GAL80^{ts}*) were shifted to 29-30ºC for 48 hours
136 before dissection. It should be noted that by crossing *UAS-GFP* to *C306-GAL4*, we observed the
137 expression of GFP in polar cells in stage 10, but not stage 9 egg chambers (data not shown). For
138 *Rab11-RNAi* experiment, crosses were maintained at 18ºC and 2-3-day-old males and females
139 with the appropriate genotype (*GR1-GAL4>UAS-mCherry-RNAi, UAS-GAL80ts or GR1-*
140 *GAL4>UAS-Rab11-RNAi, UAS-GAL80ts*) were collected and reared at 29ºC-30ºC overnight
141 before dissection. *Rab5-YFP* or *Rab11-YFP* 1-2-day old females and males were collected and
142 reared at 25ºC on fresh food sprinkled with yeast for five days before dissection. For the *Rab5^{DN}*
143 experiment, crosses were maintained at 25ºC, and 1-2-day-old females were mated to sibling
144 males and maintained at 29-30ºC for 3 days before dissection.
145
146 *Egg aspect ratio measurements*

147 Stage 14 egg chambers were selected for analysis based on the overall morphology of the egg
148 and the absence of nurse cells nuclei by DAPI staining. Stage 14 egg chambers that have
149 irregular edges or touch other egg chambers were excluded from the analysis to prevent
150 inaccurate measurements. Egg length (anterior-posterior) and width (dorsal-ventral) were
151 measured using the ImageJ/Fiji (http://fiji.sc) (Schindelin *et al*. 2012) straight-line tool, and
152 aspect ratio was calculated as length divided by width using Excel Microsoft.
153
154 *Border cell migration quantification*
155 Stage 10 egg chambers were identified based on the morphology of the egg (oocyte occupies half
156 the egg chamber, whereas the other half is occupied by the nurse cells and centripetal cells). We
157 used the GFP signal in Slbo-GAL4 crosses and DAPI and/or Fas3 staining in c306-GAL4
158 crosses to identify the location of the cluster in stage 10 egg chambers. The location of the border
159 cell cluster was quantified and grouped into four categories - complete, incomplete, failed
160 migration - based on the location of the cluster relative to the oocyte in a stage 10 egg chamber
161 (Figure 6) and disassociated cluster. In some cases, border cell clusters display two phenotypes
162 such as complete and dissociated. In this case, we quantified both phenotypes in one egg
163 chamber.
164
165 *Immunostaining and image acquisition*
166 Ovaries were dissected in 1X Phosphate-buffered saline (PBS), fixed in 4% Paraformaldehyde
167 for 20 minutes, washed three times in 1X PBS, and then permeabilized in a block solution (1X
168 PBS + 0.1% Triton + 1% Normal Donkey Serum) for 30 minutes before incubation with primary
169 antibodies either overnight at 4ºC or 2-4 hours at room temperature (~23-25ºC). The following

170 antibodies were used at the given dilutions: guinea pig (gp) anti-Cont 1:2000 *(Faivre-Sarrailh et*
171 *al*. 2004) and rabbit (rab) anti-Nrx-IV 1:500 (Stefan Baumgartner *et al*. 1996) obtained from
172 Manzoor Bhat, University of Texas Health Science Center, San Antonio, TX, gp anti-Mcr
173 1:1000 (Hall *et al*. 2014), rat anti- *D*E-cad (DCAD2) obtained from the Developmental Studies
174 Hybridoma Bank (DSHB) at the University of Iowa, Iowa City, IA 1:27, mouse (m) anti-Cora
175 (C566.9 and C615.16 mixed 1:1, DSHB) 1:50, m anti-Fas3 (7G10, DSHB) 1:260, and m anti-Sxl
176 (M18, DSHB) 1:10. DAPI (1mg/ml) was used at a dilution of 1:1000. Rab anti-GFP (290-50,
177 abcam) was used at 1:1000. Secondary antibodies were obtained from Jackson ImmunoResearch
178 Laboratories (West Grove, Pennsylvania, USA) and were used at 1:500.
179 Images were acquired using an Olympus FV1000 confocal microscope equipped with
180 Fluoview software (version 4.0.3.4). Objectives used included an UPLSAPO 20X Oil (NA:0.85),
181 a PLAPON 60X Oil (NA: 1.42), and an UPLSAPO 100X Oil (NA:1.40). Stage 14 egg chambers
182 were imaged using on Nikon Eclipse 80*i* compound microscope. Raw images were rotated and
183 cropped in ImageJ/Fiji. Micrographs were adjusted for brightness using Adobe Photoshop 21.1.1
184 (San Jose, CA). Adobe Illustrator 24.1 was used to compile the figures.
185
186 *Statistical Analysis*
187 An unpaired *t*-test was used to calculate the P values in egg chamber aspect ratio between control
188 and SJ mutant stage 14 egg chambers using GraphPad Prism 8 (https://www.graphpad.com)
189 (version 8.4.2).
190
191 *Data Availability*

192 Fly stocks are available upon request. Supplemental files are available at FigShare. Figure
193 S1shows the expression of Contactin during border cell migration. Figure S2 shows the
194 expression of Nrx-IV during border cell migration. Figure S3 shows the expression of Coracle
195 during border cell migration. The authors affirm that all the data necessary for confirming the
196 conclusions of the article are present within the article and figures.
197

198 **Results**

199

200 *Septate junction proteins are expressed in follicle cells throughout oogenesis*

201 While a few SJ *proteins* have previously been reported to be expressed in the *Drosophila*
202 ovary (Wei *et al.* 2004; Schneider *et al.* 2006; Hall *et al.* 2014; Maimon *et al.* 2014; Felix *et al.*
203 2015; Ben-Zvi and Volk 2019), a thorough analysis of their tissue distribution and subcellular
204 localization throughout oogenesis is lacking. We therefore examined the spatial and temporal
205 expression of four SJ proteins: Mcr, Cont, Nrx-IV and Cora (Fehon *et al.* 1994;Baumgartner *et*
206 *al.* 1996; Faivre-Sarrailh *et al.* 2004; Bätz *et al.* 2014; Hall *et al.* 2014). These four proteins are
207 core components of the junction for which well-characterized antibodies are available.

208 At early stages of oogenesis (stage 1-8), Mcr, Cont, and Nrx-IV all localize in puncta at the
209 lateral membrane of follicle cells and nurse cells, and show a punctate distribution in these cells
210 (Figure 1D-F). Mcr, Cont, and Nrx-IV are also more strongly expressed in polar cells (PCs) than
211 the surrounding follicle cells (asterisks in Figure 1D-F). Cora is more uniformly localized along
212 the lateral membrane of the FCs, including the PCs (Figure 1G and data not shown). We also
213 find that all of these SJ proteins are expressed in stalk cells (arrowheads in Figure 1 D and E and
214 data not shown). At stage 10b, Mcr, Nrx-IV, Cont and Cora become gradually enriched at the
215 apical-lateral membrane of the FCs just basal to the AJ (arrows in Figure 2B, D, F, and H). The
216 apical-lateral enrichment of Mcr, Cont, Nrx-IV and Cora coincides with the maturation of the SJ
217 in the FCs based upon ultrastructural analysis (Mahowald 1972; Müller 2000), and so we will

218 refer to this region as the presumptive SJ. Finally, all of these SJ proteins continue to be
219 expressed in the FCs until stage 14 of oogenesis (Figure 2C, E, G and I).
220
221 *Septate junction proteins have distinct expression patterns in the germarium*
222 The most anterior region of each ovariole is the germarium. The germarium consists of three
223 regions (only region 1 and 2 are shown in Figure 3A). Region 1 is occupied by 2-3 germline
224 stem cells (GSCs) (Figure 3A). Each GSC is in close contact with two subpopulations of somatic
225 cells - cap cells and terminal filament cells. A GSC undergoes an asymmetric cell division giving
226 rise to a daughter cell that retains its stem cell characteristics and a cystoblast cell capable of
227 differentiation (Figure 3A). The cystoblast cell divides four times forming a 2-, 4-, 8-,and 16-cell
228 cysts while being encapsulated by escort cells (ESCs). As the 16-cell cyst progresses posteriorly
229 through region 2b of the germarium, it acquires pre-follicle cells derived from a pair of follicle
230 stem cells, which will generate the FE of the newly formed egg chamber (Figure 3A) (Spradling
231 *et al.* 1997; Kirilly and Xie 2007).
232 Consistent with our previous findings, Mcr is expressed at high levels in the anterior region of
233 the germarium (Hall *et al.* 2014). To determine which cell types Mcr is expressed in, we co-
234 stained the germarium with an antibody against Sex lethal (Sxl), which is an RNA-binding
235 protein expressed in the GSCs, cystoblasts, and 2-cell cysts (Bopp *et al.* 1991; Bopp *et al.*1993).
236 Co-localization reveals that Mcr is expressed in both GSCs (asterisks in Figure 3B-B'),
237 cystoblasts (arrow in Figure 3B-B'), and the developing cystocytes (arrowhead in Figure 3B-B').
238 Cont, in contrast, shows puncta staining throughout the germarium and is not specifically
239 enriched in any cell type (Figure 3C-C'). Interestingly, Nrx-IV outlines the outside membrane of
240 the terminal filaments (arrow in Figure 3D), as well as region 1 and 2a of the germarium

241 (arrowheads in Figure 3D-D') in 5 out of 7 germaria examined. Cora is found in the escort cells
242 (yellow arrows in Figure 3 E-E'), consistent with previous studies (Maimon *et al.* 2014; Ben-Zvi
243 and Volk 2019). Cora is also expressed in the terminal filaments (white arrow) and cap cells
244 (arrowhead) (Figure 3 E-E').
245
246 *SJ proteins are required for egg elongation and dorsal appendage morphogenesis*
247 Given our findings that these four SJ proteins are expressed in the FE throughout oogenesis,
248 and our previous studies indicating a role for SJ proteins in morphogenesis, we wondered
249 whether SJ proteins might be required for morphogenetic processes in the FE. The FE plays
250 critical roles in shaping the egg chamber and producing the dorsal appendage, while a subset of
251 FE cells participates in border cell migration to form the micropyle (Montell 2003; S. Horne-
252 Badovinac 2020). Because SJ mutant animals die during embryogenesis, we used the *GAL4*
253 *UAS-RNAi* system to knock-down the expression of SJ proteins in the FCs (Brand and Perrimon
254 1993). To knock down expression of SJ proteins throughout the majority of oogenesis, we used
255 *GR1-GAL4*, which is expressed in the FCs from stage 4 to 14 of oogenesis (Gupta and
256 Schüpbach 2003; Wittes and Schüpbach 2018). In all, we tested six different SJ genes (*Cont*,
257 *cora*, *Mcr*, *lac*, *Nrx-IV*, and *sinu*). To examine overall egg chamber shape, we dissected stage 14
258 egg chambers from females expressing *SJ-RNAi* under the control of *GR1-GAL4*, imaged them
259 on a compound microscope, and determined the aspect ratio of the egg chambers using
260 measurements of egg chamber length and width using ImageJ/Fiji. Control stage 14 egg
261 chambers (*GR1-GAL4>UAS-GFP*) had a mean aspect ratio of 2.3 (Figure 4A and J). In contrast,
262 the aspect ratio of stage 14 egg chambers from all *GR1-GAL4>SJ-RNAi* is statistically
263 significant than control egg chambers (aspect ratios from 1.7 to 2.1; Figure 4B-G and J). All *SJ-*

264 *RNAi* egg chambers are significantly shorter than control (Figure 4H), and all but *Mcr-RNAi* and
265 *Cont-RNAi* are also wider than control egg chamber (Figure 4I).
266 Further examination of stage 14 SJ mutant egg chambers revealed defects in dorsal appendage
267 morphogenesis. Dorsal appendages are tubular respiratory structures that form from two
268 populations of the dorsal FE known as floor and roof cells (Figure 1A) (Duhart *et al.* 2017). The
269 primary phenotypes we observed in the *SJ-RNAi*-expressing egg chambers were either missing
270 dorsal appendages, or appendages that appeared to be broken or excessively short (Figure 4L). In
271 quantifying these phenotypes, we found that 52% of *Mcr-RNAi-,* 15% of *Cora-RNAi-*, 19% of
272 *Cont-RNAi-*, and 13% of *Lac-RNAi*-expressing egg chambers have either missing or broken
273 dorsal appendages (Figure 4M). We did not observe these phenotypes in either *Nrx-IV-RNAi-* or
274 *Sinu-RNAi*-expressing egg chambers (Figure 4M).
275
276 *SJ proteins are expressed in polar and border cells and are required for effective border cell*
277 *migration*
278 The observation that Mcr, Cont, and Nrx-IV are strongly expressed in PCs and in all FCs
279 (Figure 1D-F), motivated us to investigate their expression during the process of border cell
280 migration. Border cell migration occurs during stages 9-10 of oogenesis (Figure 5A). During
281 stage 9, signaling from the anterior PCs recruits a group of 4-8 adjacent FCs to form a cluster
282 and delaminate apically into the egg chamber. The border cell cluster is organized with a pair of
283 PCs in the center surrounded by border cells (BCs). This cluster of cells migrates between the
284 nurse cells until they reach the anterior side of the oocyte (Figure 5A). This process takes
285 approximately 4-6 hours and is complete in wild type egg chambers by stage 10 of oogenesis
286 (Prasad and Montell 2007). The border cell cluster, along with the migratory centripetal cells,

287 collaborate to form the micropyle, a hole through which the sperm enters the egg (reviewed in
288 Montell 2003; Horne-Badovinac 2020). Previous studies show that Cora and Nrg are expressed
289 in the PCs during their migration (Wei *et al.* 2004; Felix *et al.* 2015). To determine if other SJ
290 proteins are also expressed during border cell migration, we stained stage 9-10 wild type egg
291 chambers with antibodies against Mcr, Cont, and Nrx-IV. We also examined the subcellular
292 localization of Cora in the border cell cluster. To mark the PCs, we co-stained the egg chambers
293 with Fasciclin 3 (Fas3; (Snow *et al.* 1989; Khammari *et al.* 2011). We find Mcr, Cont, Nrx-IV
294 and Cora are all expressed in border cell clusters throughout their migration (Figure 5B-D and
295 Supplemental Figures 1-3). Interestingly, the expression of these SJ proteins in PCs appears
296 highest at the interfaces between PCs-BCs (Figure 5B-D and Figures S1-3). SJ protein
297 expression is also asymmetric in the border cell cluster, with higher expression along border cells
298 closest to the oocyte, suggesting that they may mark the leading edge of the migrating cluster
299 (red arrows in Figure 5B"-D").
300 Given that Mcr, Cont, Nrx-IV, and Cora are expressed in border cell clusters throughout
301 border cell migration, we wondered if they are also required for some aspect of this process. To
302 address this issue, we used *Slbo-GAL4* (Ogienko *et al.* 2018) to express RNAi against individual
303 SJ genes specifically in border cells and analyzed the border cell clusters at stage 10 in these
304 ovaries. We noticed a range of defective migration phenotypes in these egg chambers and
305 classified them into three non-exclusive groups: failed, incomplete and dissociated clusters.
306 Complete migration (e.g. arrow in Figure 6C) is characterized by having the entire border cell
307 cluster near or physically touching the oocyte by the end of stage 10. A failed cluster (e.g. arrow
308 in Figure 6D) is characterized by the inability of the border cell cluster from delaminating from
309 the FE by stage 10. An incomplete migration phenotype (e.g. arrow in Figure 6E, two dashed

310 lines indicate the range of distance at which border cell cluster was categorized as incomplete) is
311 seen as an intact cluster that has not reached the oocyte by the end of stage 10. Finally, a
312 dissociated cluster phenotype (e.g. arrow in Figure 6F) is noted as a cluster that has broken into a
313 linear string of border cells or that has one or more border cells that remain between NCs that are
314 not connected to the larger border cell cluster (compare border cell cluster in Figure 6H to an
315 intact control cluster in Figure 6H).

316 In control (*Slbo-GAL4; UAS-mCD8-GFP/UAS-mCherry-RNAi*) stage 10 egg chambers, 86%
317 (n=81) of border cell clusters completed their migration, with the remainder showing incomplete
318 migration (Figure 6I). In contrast, stage 10 egg chambers expressing RNAi against *Cora*, *Nrx-IV,*
319 or *Cont* in the border cells resulted in 58% (n=67), 50% (n=74), and 40% (n=85) of border cell
320 clusters completing migration, respectively (Figure 6I). The remaining *Cora-RNAi*- and *Nrx-IV-*
321 *RNAi*-border cell clusters showed a combination of incomplete migration or failed to delaminate
322 (Figure 6I). *Cont-RNAi*-border cell clusters also showed 35% of incomplete border cell
323 migration, but additionally had 17% of the clusters disassociating during their migration (Figure
324 6I). *Mcr-RNAi*-border cell clusters were indistinguishable from controls with 86% (n=94)
325 completing their migration and the remainder showing only 13% incomplete migration (Figure
326 6I).

327 To extend these studies, we examined border cell migration in egg chambers expressing
328 RNAi against SJ genes using the *C306-GAL4* driver that is expressed in the border cells
329 throughout the process of border cell migration (Murphy and Montell 1996) and in PCs just at
330 stage 10 (H.A., unpublished observation). In control (*C306-GAL4/UAS-Dcr; GAL80*^{ts}/+) egg
331 chambers, 78% (n=91) of BC clusters completed their migration and 19% display incomplete
332 migration (Figure 6J). Stage 10 egg chambers expressing RNAi against *Mcr* in border and polar

333 cells resulted in 66% (n=98) complete border cell migration with 30% showing incomplete
334 migration, 5% dissociated and 3% failed border cell cluster (Figure 6J). Similarly, egg chambers
335 expressing *Nrx-RNAi* in border and polar cells show 66% (n=59) complete border cell migration
336 with 30% showing incomplete migration and 3% failing to delaminate (Figure 6J). Finally, 78%
337 (n=70) of stage 10 *Cora-RNAi*-expressing border and polar cells show complete border cell
338 migration, whereas 20% show incomplete migration and 3% fail to delaminate (Figure 6J).
339
340 *SJ biogenesis in the follicular epithelium*
341 The redistribution of SJ proteins in the FCs of later stage egg chambers resembles the
342 dynamic relocalization of SJ proteins during the biogenesis of the junction during embryogenesis
343 (Tiklová *et al*. 2010). In embryonic epithelia, SJ protein enrichment at the apical-lateral domain
344 (presumptive SJ) requires endocytosis and recycling of SJ proteins to the membrane, and is
345 interdependent on the presence of all core SJ proteins (Ward *et al.* 1998; Hall *et al.* 2014).
346 Coincident with the strong localization of SJ proteins to the presumptive SJ at stage 16 of
347 embryogenesis, ladder-like electron-dense intermembrane septae are visible by electron
348 microscopy that become progressively organized by stage 17 (Schulte *et al.* 2003; Hildebrandt *et*
349 *al.* 2015). We therefore sought to determine if similar processes occurred in the FE.
350 To test for the interdependence of SJ proteins for localization, we examined Cora and Mcr
351 expression in wild type, *Mcr-RNAi*, and *Nrx-IV-RNAi* stage 12 FCs. Whereas Cora is strongly
352 co-localized with Mcr at the apical-lateral domain of the FCs of wild type stage 12 egg chambers
353 (n=95 cells, 31 egg chambers) (Figure 7A), Cora and Mcr are mislocalized along the lateral
354 domain in *Nrx-IV-RNAi* FCs (Figure 7B), much like they do in earlier stage FCs (Figure 1D).
355 Specifically, we observed 6 out of 20 cells examined in 19 egg chambers that showed complete

356 mislocalization and 13 out of these 20 cells showing lateral localization with some degree of
357 apical enrichment. Similarly, in stage 12 *Mcr-RNAi* FCs, Cora is mislocalized along the lateral
358 membrane in 39 out of 47 cells examined from 19 egg chambers, with the remaining 8 cells
359 showing some enrichment of Cora at the apical lateral domain (Figure 7C). Notably, cells that
360 showed apical enrichment of Cora also retained small foci of Mcr expression that overlaps with
361 the enriched Cora (Figure 7D), suggesting the perdurance of Mcr in these cells may have allowed
362 for normal SJ organization. Together, these experiments indicate that SJ biogenesis in the
363 follicular epithelium of late stage egg chambers requires the expression of at least some core SJ
364 proteins.

365 We next wanted to investigate whether the relocalization of SJ proteins to the presumptive SJ
366 required endocytosis and recycling. In the embryonic hindgut, Cora, Gliotactin (Glio), Sinu, and
367 Melanotransferrin (Mtf) localize with the early endosomal marker, Rab5, and partially localize
368 with the recycling marker, Rab11 during SJ biogenesis (Tiklová *et al.* 2010). Moreover, blocking
369 Rab5 or Rab11 function prevents Cora, Glio, Sinu, and Mtf apical-lateral localization (Tiklová *et*
370 *al.* 2010), and thus SJ formation. To determine if the redistribution of SJ proteins in the FCs is
371 mediated by Rab5 and Rab11, we first asked whether Mcr co-localized with Rab5 and
372 Rab11compartments in stage 10 FCs. We chose to analyze stage 10 egg chambers because this is
373 the stage that immediately precedes Mcr's re-localization to the presumptive SJ (similar to stage
374 13/14 of embryogenesis). During stage 10 of oogenesis, we find that Mcr still localizes
375 uniformly along the lateral (and to the apical membrane), but is also found in punctate
376 intracellular compartments (Figure 8A-A''). Notably, some of these Mcr positive puncta co-
377 localize with Rab5-YFP puncta, suggesting that these Mcr molecules are in early endosomes. We
378 noted less colocalization of Mcr puncta with Rab11-YFP-positive puncta, although we did find

379 some examples of co-localization (Figure 8B-B''). To determine if the co-localization of Mcr
380 and Rab5 have functional significance, we expressed a dominant negative Rab5 (*UAS-Rab5^{DN}*)
381 in the FCs using *GR1-GAL4* and examined the expression of Mcr and Cora in stage 11 FCs. In
382 wild-type FCs at that stage, Mcr and Cora are enriched at the apical-lateral membrane (n=91
383 cells, 15 egg chambers) (arrows in Figure 8 C), whereas both Mcr and Cora remains localized
384 along the lateral membrane in the Rab5^{DN}-expressing FCs (n=97 cells, 15 egg chambers) (Figure
385 8D). Similarly, Cora and Mcr co-localize at the apical-lateral membrane of the FCs of stage 12
386 egg chambers (n=64 cells, 15 egg chambers) (arrows in Figure 8E), whereas knocking down the
387 expression of Rab11 in stage 12 FCs results in the lateral localization of Mcr and/or Cora (n=23
388 cells out of 44, 16 egg chambers) (arrow in Figure 8F). Interestingly, we observed *Rab11-RNAi*
389 expressing cells in which Cora is mislocalized laterally and Mcr is completely missing from the
390 plasma membrane (n=21 cells out of 44, 16 egg chambers) (arrowhead in Figure 8F-F''),
391 suggesting that Mcr may have been endocytosed and shunted for degradation since it could not
392 be recycled. Taken together, these results suggest that similar to embryonic epithelia, the
393 maturation of SJs in the follicular epithelium requires Rab5-mediated endocytosis and Rab11-
394 mediated recycling.
395

396 **Discussion**

397

398 In this study, we have demonstrated that a subset of SJ proteins are expressed in egg chambers
399 throughout oogenesis and are required for critical morphogenetic processes that shape the egg,
400 including egg chamber elongation, dorsal appendage formation and border cell migration
401 (required to form the micropyle). Interestingly, the subcellular localization of these SJ proteins in

402 the ovarian FCs changes coincident with the establishment of the occluding junction in much the
403 same way that they do during embryogenesis in ectodermal epithelial cells (Tiklová *et al.* 2010),
404 suggesting that a similar maturation process for the SJ occurs in this tissue.
405
406 *Biogenesis of the SJ in the FE*
407 The mechanisms of SJ biogenesis in embryonic epithelia has been well-studied and involves
408 several steps in which transmembrane SJ proteins are first localized all along lateral plasma
409 membranes (by stage 12 of embryogenesis), but then must be endocytosed and recycled back to
410 the plasma membrane prior to aggregating in the region of the presumptive SJ (between stages
411 13 and 16; (Tiklová *et al.* 2010)). Prior to this relocalization step, SJ proteins show high mobility
412 in the plane of the membrane by Fluorescence Recovery After Photobleaching (FRAP) analysis,
413 but become strongly immobile as the relocalization is occurring (Oshima and Fehon 2011). As
414 these steps are occurring (e.g. stage 14 of embryogenesis), electron-dense material begins to
415 accumulate between adjacent cells in the presumptive SJ that takes on the appearance of ladder-
416 like septae by stage 17 of embryogenesis (Tepass and Hartenstein 1994). Functional studies
417 indicate that the occluding function of the junction is established late in embryogenesis, near the
418 end of stage 15 (Paul *et al.* 2003). Importantly, the process of SJ biogenesis is interdependent on
419 the function of all core components of the junction and several accessory proteins including Rab
420 5 and Rab 11 (Ward *et al.* 1998; Genova and Fehon 2003; Tiklová *et al.* 2010).
421 Here, we observe that many of these same steps occur in the maturation of SJs in the FE. We
422 first show that SJ proteins are expressed in the FE beginning early in ovarian development where
423 they localize all along the lateral membrane (Figure 1). These proteins appear to be endocytosed
424 later in egg chamber development (Figure 8) prior to becoming enriched at the presumptive SJ

425 by stage 10b/11 (Figure 2). The relocalization of SJ proteins to the SJ requires core SJ proteins
426 including Mcr and Nrx-IV, and accessory proteins including Rab 5 and Rab 11 (Figures 7 and 8).
427 Prior studies indicate the presence of electron dense material between FE cells as early as stage 6
428 (Müller 2000), with a ladder-like appearance of extracellular septae by stage 10B (Mahowald
429 1972). A recent study of the occluding function in the FE show a similar pattern of protein
430 localization for endogenously tagged Neuroglian-YFP and Lachesin-GFP, and demonstrates that
431 an intact occluding junction is formed during stage 11 of oogenesis (Isasti-Sanchez *et al.* 2020).
432 It is interesting to note the FE is a secondary epithelium initiated by a mesenchymal to epithelial
433 transition (Tepass *et al.* 2001), and yet SJ biogenesis appears to be very similar to that observed
434 in the primary epithelia found in the embryo.
435
436 *SJ proteins are required for morphogenetic events during oogenesis*
437 The similarities in the dynamic expression of SJ proteins in the FE and embryonic epithelia,
438 coupled with the observation that SJ proteins are required for numerous embryonic
439 developmental events ((Hall *et al.* 2014) and references therein) motivated us to explore whether
440 SJ proteins have similar roles in morphogenetic processes that shape the egg. Using a targeted
441 RNAi approach, we show that reducing the expression of Mcr, Nrx-IV, Cont, Cora, Sinu, or Lac
442 throughout oogenesis in the FCs results in significantly rounder stage 14 egg chambers, with
443 many showing additional defects in dorsal appendages (Figure 4). The initiation and
444 maintenance of egg elongation is achieved at various stages throughout oogenesis (Gates 2012;
445 Bilder and Haigo 2012; Cetera and Horne-Badovinac 2015). From stage 3-8, a gradient of JAK-
446 STAT signaling is required at each pole of the egg chamber to promote Myosin II-based apical
447 cell contractions (Alégot *et al.* 2018). From stage 6-8, the formation of a robust planar polarized

448 molecular corset - consisting of basal actin cytoskeleton and basement membrane protein fibrils -
449 is required for egg elongation, and requires collective FC migration over a static basement
450 membrane (Gutzeit *et al.* 1991; Frydman and Spradling 2001; Bateman *et al.* 2001; Viktorinová
451 *et al.* 2009; Haigo and Bilder 2011; Horne-Badovinac *et al.* 2012; Cetera *et al.* 2014; Isabella
452 and Horne-Badovinac 2016; Campos *et al.* 2020). During the middle stages of oogenesis (stages
453 9 and 10), basal actin stress fibers undergo actomyosin contractions, which contribute to egg
454 elongation (He *et al*. 2010; Qin *et al*. 2017). Finally, later in oogenesis, the maintenance of a
455 planar polarized molecular corset is required to retain an elongated egg chamber shape (Haigo
456 and Bilder 2011; Cha *et al.* 2017; Campos *et al.* 2020). Future studies are needed to determine if
457 SJ proteins are required for the establishment and/or maintenance of egg shape. Since many of
458 the events involved in egg elongation occur prior to the formation of a functional (and
459 ultrastructurally intact) occluding junction, it raises the possibility that SJ proteins have a
460 function in morphogenesis that is independent of their role in forming a tight occluding junction,
461 much as they do in the embryo.
462 Our observation that specifically knocking down the expression of several SJ proteins in
463 border cells (including polar cells using *C306-GAL4*) results in defective border cell migration
464 (Figure 6) supports a role for SJ proteins in morphogenesis, independent of their role in forming
465 an occluding junction. The phenotypes we observed include failing to complete migration by the
466 end of stage 10 and partial disassociation of the complex, although it is possible that these
467 phenotypes underestimate the full requirement of SJ proteins in border cell migration since this
468 process takes a relatively short time (4-6 hours) (Prasad and Montell 2007), while SJ proteins are
469 thought to be very stable in the membrane (Oshima and Fehon 2011). Nevertheless, these
470 phenotypes may indicate a role for SJ proteins in cell adhesion or cell polarity during migration.

471 Specifically, we note that Mcr appears to be enriched in border cells along membranes that are
472 closest to the oocyte (Figure 5). Perhaps the incomplete migration defect results from a
473 meandering migration through the nurse cells. A potential role for SJ proteins in cell adhesion in
474 the ovary has been reported previously. Reducing the level of Nrg in FCs results in the failure of
475 newly divided FCs to reintegrate into the FE, indicating a role for *Nrg* in lateral cell adhesion
476 (Bergstralh *et al.* 2015). In addition, expressing a null allele of *Nrg* in FCs enhances the invasive
477 tumor phenotype of a *Discs Large* (*Dlg*) mutation (Wei *et al.* 2004).
478
479 *Unique roles for SJ proteins in the germarium*
480 Unlike the polarized FE, the germarium consists of numerous unique cell types with distinct
481 functions. Cap cells, terminal filament cells and escort cells act as a niche for germ stem cell
482 renewal and differentiation (Eliazer and Buszczak 2011; Xie and Spradling 2000). Follicle stem
483 cells also reside in the germarium to produce the FE needed to encapsulate newly formed germ
484 cell cysts. It is interesting that Mcr, Cont, Nrx-IV, and Cora all show distinct expression pattern
485 within the germarium (Figure 3). For example, Cora is enriched in cap cells, terminal filament
486 cells and escort cells, whereas Nrx-IV outlines the outside membrane of region 1 and 2a of the
487 germarium. Mcr is highly expressed in the germ line stem cells, the cystoblasts and cystocytes
488 (Figure 3). This location-specific expression of SJ proteins provides a useful tool to identify
489 different cell types using antibodies against SJ proteins as markers.
490 In the *Drosophila* testes, Nrx-IV and Cora are expressed and are required for germ stem cell
491 differentiation by forming a permeability barrier at a late stage of spermatogenesis (Fairchild *et*
492 *al.* 2015). Additionally, Duby *et al.* showed that a total of five SJ proteins, including Nrx-IV and
493 Cora, co-localize with Dlg at the germline-somatic cell interfaces during the early and late

494 spermatogenesis (Dubey *et al*. 2019). It is unclear whether a similar permeability barrier is
495 established in the germarium, but the non-overlapping expression of SJ proteins in the
496 germarium argues against a SJ-like occluding function and instead suggests unique roles for
497 these proteins in aspects of early egg chamber development. For example, Nrx-IV and Cora are
498 expressed in cells/regions that are known to provide a niche for GSCs, suggesting a role for these
499 proteins in germline maintenance and differentiation, whereas Mcr may play a role in
500 maintaining cell-cell adhesion to regulate germline cell division and differentiation. Thus, future
501 studies could be aimed at identifying these unique functions as well as uncovering common
502 mechanisms by which SJ proteins facilitate morphogenetic processes during development.
503

504 **Acknowledgements**
505 We thank Jocelyn McDonald, the Bloomington *Drosophila* Stock Center, and the Vienna
506 *Drosophila* RNAi Center for fly stocks. We thank Manzoor Bhat and the Developmental Studies
507 Hybridoma Bank (created by the NICHD of the NIH and maintained at The University of Iowa,
508 Department of Biology, Iowa City, IA 52242) for antibodies used in this study. We thank Brian
509 Ackley for the use of his Olympus FV1000 confocal microscope. We thank Lindsay Ussher for
510 preliminary studies on border cell migration and thoughtful discussions on the project. We also
511 thank Sally Horne-Badovinac, Jocelyn McDonald, Yujun Chen, and members of the Ward lab
512 for helpful discussion about the project and manuscript.

513 **References:**

514 Alégot, H., P. Pouchin, O. Bardot, and V. Mirouse. 2018. Jak-Stat pathway induces Drosophila
515 follicle elongation by a gradient of apical contractility. *ELife* 7: 1–21.
516 https://doi.org/10.7554/elife.32943.

517 Banerjee, S, R. J. Bainton, N. Mayer, R Beckstead, and M. A. Bhat. 2008. Septate junctions are
518 required for ommatidial integrity and blood-eye barrier function in Drosophila. *Nature* 23:
519 1–7. https://doi.org/10.1038/jid.2014.371.

520 Bateman, Jack, R. Srekantha Reddy, Haruo Saito, and David Van Vactor. 2001. The receptor
521 tyrosine phosphatase dlar and integrins organize actin filaments in the Drosophila follicular
522 epithelium. *Curr Biol* 11: 1317–27. https://doi.org/10.1016/S0960-9822(01)00420-1.

523 Bätz, T., D. Förster, and S. Luschnig. 2014. The transmembrane protein macroglobulin
524 complement-related is essential for septate junction formation and epithelial barrier function
525 in Drosophila. *Development* 141: 899–908. https://doi.org/10.1242/dev.102160.

526 Baumgartner, S., J. T. Littleton, K. Broadie, M. A. Bhat, R. Harbecke *et al.,* 1996. A Drosophila
527 neurexin is required for septate junction and blood-nerve barrier formation and function.
528 *Cell* 87: 1059–68. https://doi.org/10.1016/S0092-8674(00)81800-0.

529 Behr, M., D. Riedel, and R. Schuh. 2003. The claudin-like megatrachea is essential in septate
530 junctions for the epithelial barrier function in Drosophila. *Dev Cell* 5: 611–620.
531 https://doi.org/10.1016/S1534-5807(03)00275-2.

532 Ben-Zvi, D. S., and T. Volk. 2019. Escort cell encapsulation of Drosophila germline cells Is
533 maintained by irre cell recognition module proteins. *Biol Open* 8.
534 https://doi.org/10.1242/bio.039842.

535 Bilder, D., and S. L. Haigo. 2012. Expanding the morphogenetic repertoire: rerspectives from the

536 Drosophila egg. *Dev Cell* 22: 12–23. https://doi.org/10.1016/j.devcel.2011.12.003.
537 Bopp, D., L. R. Bell, T. W. Cline, and P. Schedl. 1991. Developmental distribution of female-
538 specific sex-lethal proteins in Drosophila melanogaster. *Genes Dev* 5: 403–15.
539 https://doi.org/10.1101/gad.5.3.403.
540 Bopp, D., J. I. Horabin, R. A. Lersch, T. W. Cline, and P. Schedl. 1993. Expression of the sex-
541 lethal gene Is controlled at multiple levels during Drosophila oogenesis. *Development* 118:
542 797–812.
543 Brand, A. H., and N. Perrimon. 1993. Targeted gene expression as a means of altering cell fates
544 and generating dominant phenotypes. *Development* 118: 401–15.
545 Campos, F. C., C. Dennis, H. Alégot, C. Fritsch, A. Isabella *et al*., 2020. Oriented basement
546 membrane fibrils provide a memory for f-actin planar polarization via the Dystrophin-
547 Dystroglycan complex during tissue elongation. *Development* 147 (7).
548 https://doi.org/10.1242/dev.186957.
549 Cetera, M., and S. Horne-Badovinac. 2015. Round and round gets you somewhere: collective
550 cell migration and planar polarity in elongating Drosophila egg chambers. *Curr Opin Genet*
551 *Dev* 32: 10–15. https://doi.org/10.1016/j.gde.2015.01.003.
552 Cetera, M., G. R. Ramirez-San Juan, P. W. Oakes, L. Lewellyn, M. J. Fairchild *et al*., 2014.
553 Epithelial rotation promotes the global alignment of contractile actin bundles during
554 Drosophila egg chamber elongation. *Nat Commun* 5: 5511.
555 https://doi.org/10.1038/ncomms6511.
556 Cha, I. J., J. H. Lee, K. S. Cho, and S. B. Lee. 2017. Drosophila tensin plays an essential role in
557 cell migration and planar polarity formation during oogenesis by mediating integrin-
558 dependent extracellular signals to actin organization. *Biochem and Biophys Res Commun*

559 484: 702–9. https://doi.org/10.1016/j.bbrc.2017.01.183.
560 Dubey, P., T. Kapoor, S. Gupta, S. Shirolikar, and K. Ray. 2019. Atypical septate junctions
561 maintain the somatic enclosure around maturing spermatids and prevent premature sperm
562 release in Drosophila testis. *Biol Open* 8: bio036939. https://doi.org/10.1242/bio.036939.
563 Duhart, J. C., T. T. Parsons, and L. A. Raftery. 2017. The repertoire of epithelial morphogenesis
564 on display: progressive elaboration of Drosophila egg structure. *Mech Dev*. 148: 13-39.
565 https://doi.org/10.1016/j.mod.2017.04.002.
566 Eliazer, S., and M. Buszczak. 2011. Finding a niche: studies from the Drosophila ovary. *Stem*
567 *Cell Res Ther*. 2:45. https://doi.org/10.1186/scrt86.
568 Fairchild, M. J., C. M. Smendziuk, and G. Tanentzapf. 2015. A somatic permeability barrier
569 around the germline is essential for Drosophila spermatogenesis. *Development* 142: 268–81.
570 https://doi.org/10.1242/dev.114967.
571 Faivre-Sarrailh, C., S. Banerjee, J. Li, M. Hortsch, L. Monique *et al*., 2004. Drosophila contactin,
572 a homolog of vertebrate contactin, is required for septate junction organization and
573 paracellular barrier function. *Development* 131: 4931–42.
574 https://doi.org/10.1242/dev.01372.
575 Fehon, R. G., I. A. Dawson, and S. Artavanis-Tsakonas. 1994. A *Drosophila* homologue of
576 membrane-skeleton protein 4.1 is associated with septate junctions and is encoded by the
577 coracle gene. *Development* 120: 545–57. https://doi.org/10.1083/jcb.120.1.129.
578 Felix, M., M. Chayengia, R. Ghosh, A. Sharma, and M. Prasad. 2015. Pak3 regulates apical-
579 basal polarity in migrating border cells during Drosophila oogenesis. *Development* 142:
580 3692–3703. https://doi.org/10.1242/dev.125682.
581 Frydman, H. M., and A. C. Spradling. 2001. The receptor-like tyrosine phosphatase lar is

582 required for epithelial planar polarity and for axis determination within Drosophila ovarian
583 follicles. *Development* 128: 3209–20.
584 Gates, J. 2012. Drosophila egg chamber elongation: insights into how tissues and organs are
585 shaped." *Fly* 6: 213–27. https://doi.org/10.4161/fly.21969.
586 Genova, J. L., and R. G. Fehon. 2003. Neuroglian, gliotactin, and the Na+/K+ ATPase are
587 essential for septate junction function in Drosophila. *J of Cell Biol* 161: 979–89.
588 https://doi.org/10.1083/jcb.200212054.
589 Gupta, T., and T. Schüpbach. 2003. Cct1, a phosphatidylcholine biosynthesis enzyme, is required
590 for Drosophila oogenesis and ovarian morphogenesis." *Development* 130: 6075–87.
591 https://doi.org/10.1242/dev.00817.
592 Gutzeit, H. O, W. Eberhardt, and E. Gratwohl. 1991. Laminin and basement membrane-
593 associated microfilaments in wild-type and mutant Drosophila ovarian follicles. *J Cell Sci*
594 100: 781–88.
595 Haigo, S. L., and D. Bilder. 2011. Global tissue revolutions in a morphogenetic movement
596 controlling elongation. *Science* 331: 1071–74. https://doi.org/10.1126/science.1199092.
597 Hall, S., C. Bone, K. Oshima, L. Zhang, M. McGraw *et al*., 2014. Macroglobulin complement-
598 related encodes a protein required for septate junction organization and paracellular barrier
599 function in Drosophila. *Development* 141: 889–98. https://doi.org/10.1242/dev.102152.
600 Hall, S., and R. E. Ward. 2016. Septate junction proteins play essential roles in morphogenesis
601 throughout embryonic development in Drosophila." *G3* 6: 2375–84.
602 https://doi.org/10.1534/g3.116.031427.
603 He, L., X. Wang, H. L. Tang, and D. J. Montell. 2010. Tissue elongation requires oscillating
604 contractions of a basal actomyosin network. *Nat Cell Biol* 12:1133-1142.

605 https://doi.org/10.1038/ncb2124.

606 Hildebrandt, A., R. Pflanz, M. Behr, T. Tarp, D. Riedel, and R. Schuh. 2015. Bark beetle
607 controls epithelial morphogenesis by septate junction maturation in Drosophila. *Dev Biol*
608 400: 237–47. https://doi.org/10.1016/j.ydbio.2015.02.008.

609 Horne-Badovinac, S. 2020. The Drosophila micropyle as a system to study how epithelia build
610 complex extracellular structures. *Phil Trans R Soc* 375: 20190561.
611 https://doi.org/10.1098/rstb.2019.0561.

612 Horne-Badovinac, S., and D. Bilder. 2005. Mass transit: epithelial morphogenesis in the
613 Drosophila egg chamber. *Dev Dyn* 232: 559–74. https://doi.org/10.1002/dvdy.20286.

614 Horne-Badovinac, S., J. Hill, G. Gerlach, W. Menegas *et al*., 2012. A Screen for round egg
615 mutants in Drosophila identifies tricornered, furry, and misshapen as regulators of egg
616 chamber elongation. *G3* 2: 371–78. https://doi.org/10.1534/g3.111.001677.

617 Ile, K. E., R. Tripathy, V. Goldfinger, and A. D. Renault. 2012. Wunen, a Drosophila lipid
618 phosphate phosphatase, is required for septate junction-mediated barrier function.
619 *Development* 139: 2535–46. https://doi.org/10.1242/dev.077289.

620 Isabella, A. J., and S. Horne-Badovinac. 2016. Rab10-mediated secretion synergizes with tissue
621 movement to build a polarized basement membrane architecture for organ morphogenesis.
622 *Dev Cell* 38: 47–60. https://doi.org/10.1016/j.devcel.2016.06.009.

623 Isasti-Sanchez, J., F. Munz-Zeise, and S. Luschnig. 2020. Transient opening of tricellular
624 vertices controls paracellular transport through the follicle epithelium during Drosophila
625 oogenesis. *BioRxiv*, no. CiM: 2020.02.29.971168.
626 https://doi.org/10.1101/2020.02.29.971168.

627 Ward, R. E., R. S. Lamb, and R. G. Fehon. 1998. A conserved functional domain of Drosophila

628 coracle is required for localization at the septate junction and has membrane-organizing
629 activity. *Cell* 140: 1463–73.
630 Izumi, Y., and M. Furuse. 2014. Molecular organization and function of invertebrate occluding
631 junctions. *Semin Cell Dev Bio* 36: 186–93. https://doi.org/10.1016/j.semcdb.2014.09.009.
632 Khammari, A., F. Agnès, P. Gandille, and A. M. Pret. 2011. Physiological apoptosis of polar
633 cells during Drosophila oogenesis is mediated by hid-dependent regulation of diap1. *Cell*
634 *Death and Differ*. 18: 793–805. https://doi.org/10.1038/cdd.2010.141.
635 Kirilly, D., and T. Xie. 2007. The Drosophila ovary: an active stem cell community. *Cell Res* 17:
636 15–25. https://doi.org/10.1038/sj.cr.7310123.
637 Lamb, R. S., R. E. Ward, L. Schweizer, and R. G. Fehon. 1998. Drosophila coracle, a member of
638 the protein 4.1 superfamily, has essential structural functions in the septate junctions and
639 developmental functions in embryonic and adult epithelial cells. *Mol Bio Cell* 9: 3505–19.
640 https://doi.org/10.1091/MBC.9.12.3505.
641 Mahowald, A. P. 1972. Ultrastructural observations on oogenesis in Drosophila. *J Morph* 137:
642 29–48. https://doi.org/10.1002/jmor.1051370103.
643 Maimon, I., M. Popliker, and L. Gilboa. 2014. Without children is required for stat-mediated
644 zfh1 transcription and for germline stem cell differentiation. *Development* 141: 2602–10.
645 https://doi.org/10.1242/dev.109611.
646 Montell, D. J. 2003. Border-Cell Migration: The Race Is On. *Nat Rev Mol Cell Bio* 4: 13–24.
647 https://doi.org/10.1038/nrm1006.
648 Moyer, K. E., and J. R. Jacobs. 2008. Varicose: a MAGUK required for the maturation and
649 function of Drosophila septate junctions. *BMC Dev. Bio*. 8;99. https://doi.org/10.1186/1471-
650 213X-8-99.

651 Müller, H. J. 2000. Genetic control of epithelial cell polarity: lessons from Drosophila. *Dev Dyn*
652 218: 52–67. https://doi.org/10.1002/(sici)1097-0177(200005)218:1<52::aid-
653 dvdy5>3.3.co;2-c.
654 Murphy, A. M., and D. J. Montell. 1996. Cell type-specific roles for cdc42, rac, and rhol in
655 Drosophila oogenesis. *J Cell Bio* 133: 617–30. https://doi.org/10.1083/jcb.133.3.617.
656 Nelson, K. S., M. Furuse, and G.J. Beitel. 2010. The Drosophila claudin kune-kune is required
657 for septate junction organization and tracheal tube size control. *Genetics* 185: 831–39.
658 https://doi.org/10.1534/genetics.110.114959.
659 Noirot-timothée, C., D. S. Smith, M. L. Cayer, and C. Noirot. 1978. Septate junctions in insects:
660 comparison between intercellular and intramembranous structures." *Tissue Cell* 10: 125–36.
661 https://doi.org/10.1016/0040-8166(78)90011-3.
662 Ogienko, A. A., L. A. Yarinich, E. V. Fedorova, M. O. Lebedev *et al*., 2018. New slbo-gal4
663 driver lines for the analysis of border cell migration during Drosophila oogenesis.
664 *Chromosoma* 127: 475–87. https://doi.org/10.1007/s00412-018-0676-7.
665 Oshima, K., and R. G. Fehon. 2011. Analysis of protein dynamics within the septate junction
666 reveals a highly stable core protein complex that does not include the basolateral polarity
667 protein discs large." *J Cell Sc* 124: 2861–71. https://doi.org/10.1242/jcs.087700.
668 Paul, S. M., M. Ternrt, P. Salvaterra, and G. Beitel. 2003. The Na+/K+ ATPase is required for
669 septate junction function and epithelial tube-size control in the Drosophila tracheal system.
670 *Development* 130: 4963–74. https://doi.org/10.1242/dev.00691.
671 Prasad, M., and D. J. Montell. 2007. Cellular and molecular mechanisms of border cell migration
672 analyzed using time-lapse live-cell imaging. *Dev Cell* 12: 997–1005.
673 https://doi.org/10.1016/j.devcel.2007.03.021.

674 Qin, X., B. O. Park, J. Liu, B. Chen, V. Choesmel-Cadamuro *et al*., 2017. Cell-matrix adhesion
675 and cell-cell adhesion differentially control basal myosin oscillation and Drosophila egg
676 chamber elongation. *Nat Commun*. 8: 14708. https://doi.org/10.1038/ncomms14708.
677 Schindelin, J., I. Arganda-Carreras, E. Frise, V. Kaynig, M. Longair *et al*., 2012. Fiji: an open-
678 source platform for biological-image analysis. *Nat Methods* 9: 676–82.
679 https://doi.org/10.1038/nmeth.2019.
680 Schneider, M., A.K. Khalil, J. Poulton, C. Castillejo-Lopez, D. Egger-Adam *et al*., 2006.
681 Perlecan and dystroglycan act at the basal side of the Drosophila follicular epithelium to
682 maintain epithelial organization. *Development* 133: 3805–15.
683 https://doi.org/10.1242/dev.02549.
684 Schulte, J., U. Tepass, and V. J. Auld. 2003. Gliotactin, a Novel Marker of Tricellular Junctions,
685 Is Necessary for Septate Junction Development in Drosophila. *Journal Cell Bio* 161 (5):
686 991–1000. https://doi.org/10.1083/jcb.200303192.
687 Snow, Peter M., Allan J. Bieber, and Corey S. Goodman. 1989. Fasciclin III: a novel homophilic
688 adhesion molecule in Drosophila. *Cell* 59: 313–23. https://doi.org/10.1016/0092-
689 8674(89)90293-6.
690 Spradling, A. C., M. De Cuevas, D. Drummond-Barbosa, L. Keyes, M. Lilly *et al*., 1997. The
691 Drosophila germarium: stem cells, germ line cysts, and oocytes. *Cold Spring Harb Symp*
692 *Quant Biol* 62: 25–34.
693 Tepass, U., G. Tanentzapf, R. Ward, and R. Fehon. 2001. Epithelial cell polarity and cell
694 junctions in Drosophila. *Annu Rev Gene*. 35: 747–84.
695 https://doi.org/10.1146/annurev.genet.35.102401.091415.
696 Tepass, Ulrich, and Volker Hartenstein. 1994. The development of cellular junctions in the

Drosophila embryo. *Dev Biol* 161:563-96. https://doi.org/10.1006/dbio.1994.1054.

Tiklová, K., K. A. Senti, S. Wang, A. GräCurrency Signslund, and C. Samakovlis. 2010. Epithelial septate junction assembly relies on melanotransferrin iron binding and endocytosis in Drosophila. *Nature Cell Biol*. 12: 1071–77. https://doi.org/10.1038/ncb2111.

Venema, D. R., T. Zeev-Ben-Mordehai, and V. J. Auld. 2004. Transient apical polarization of gliotactin and coracle is required for parallel alignment of wing hairs in Drosophila. *Dev Biol* 275: 301–14. https://doi.org/10.1016/j.ydbio.2004.07.040.

Viktorinová, I., T. König, K. Schlichting, and C. Dahmann. 2009. The cadherin fat2 is required for planar cell polarity in the Drosophila ovary. *Development* 136: 4123–32. https://doi.org/10.1242/dev.039099.

Ward, R. E., R. S. Lamb, and R. G. Fehon. 1998. A conserved functional domain of Drosophila coracle is required for localization at the septate junction and has membrane-organizing activity. *Cell* 140: 1463–73.

Wei, J., M. Hortsch, and S. Goode. 2004. Neuroglian Stabilizes Epithelial Structure during Drosophila Oogenesis. *Dev. Dyn*. 230: 800–808. https://doi.org/10.1002/dvdy.20108.

Wittes, J., and T. Schüpbach. 2018. A gene expression screen in Drosophila melanogaster identifies novel JAK/STAT and EGFR targets during oogenesis. *G3* 9: 47–60. https://doi.org/10.1534/g3.118.200786.

Wu, V. M., J. Schulte, A. Hirschi, U. Tepass, and G.J. Beitel. 2004. Sinuous is a Drosophila claudin required for septate junction organization and epithelial tube size control. *J Cell Biol*. 164: 313–23. https://doi.org/10.1083/jcb.200309134.

Wu, V. M., M. H. Yu, R. Paik, S. Banerjee, Z. Liang *et al*., 2007. Drosophila varicose, a member of a new subgroup of basolateral MAGUKs, is required for septate junctions and tracheal

720 morphogenesis. *Development* 134: 999–1009. https://doi.org/10.1242/dev.02785.
721 Xie, T., and A. C. Spradling. 2000. A niche maintaining germ line stem cells in the Drosophila
722 ovary. *Science* 290: 328–30. https://doi.org/10.1126/science.290.5490.328.
723
724
725 **Figure Legends**
726
727 **Figure 1. Mcr, Cont, Nrx-IV, and Cora expression during early stages of oogenesis.** (A)
728 Diagram of a female *Drosophila* ovariole. Egg chambers are formed in the most anterior region
729 of the ovariole called the germarium (Germ). Each egg chamber undergoes 14 developmental
730 stages while connecting to each other through stalk cells (SCs) to form a mature stage 14 egg.
731 (B) Diagram of a stage 8 egg chamber. An egg chamber consists of 15 nurse cells (NCs) and one
732 oocyte (Oo.), which are surrounded by a monolayer of follicle cells (FCs). At the anterior and
733 posterior ends of an egg chamber resides a pair of differentiated FCs called polar cells (PCs). (C)
734 Diagram of the follicular epithelium in a stage 10b egg chamber. FCs have defined apical-basal
735 polarity with the apical surface facing the germline. By stage 10b the septate junction (SJ) has
736 formed along the lateral membrane. At that stage, the junctional complex consists of a marginal
737 zone (MZ), an adherens junction (AJ), and a SJ. (D-G) Confocal optical sections of wild type
738 early stages egg chambers stained with antibodies against Mcr (D and single channel in D'),
739 Cont (E and E'), Nrx-IV (F and F'), and Cora (G and G'), and co-stained with antibodies against
740 Ecad (green) and labeled with DAPI. All four SJ proteins are expressed throughout the egg
741 chamber along FC membranes and in the NCs. Mcr, Cont, and Nrx-IV (D-F) are found along the
742 membrane and in puncta, whereas Cora is found predominantly at the membrane (G). In

743 addition, Mcr, Cont, and Nrx-IV are highly expressed in the PCs (asterisks in D-F), whereas
744 Cora is expressed in these cells with same level of expression relative to the follicle cells (data
745 not shown). Anterior is to the left in each ovariole. Scale bar= 25µm.
746
747 **Figure 2. Mcr, Cont, Nrx-IV, and Cora localization at later stages of oogenesis.** (A) Diagram
748 of a stage 12 egg chamber, showing the area where confocal images were taken in panels B, D, F
749 and H (red box) which is the boundary between the oocyte (Oo.) and nurse cells (NCs). Confocal
750 optical sections of wild type stage 11 – 12 egg chambers (B, D, F, and H) or stage 14 (C, E, G,
751 and I) stained with antibodies against Mcr (B and C), Cont (D and E), Nrx-IV (F and G), or Cora
752 (H and I) and co-stained with antibodies against Ecad (green) and labeled with DAPI (blue).
753 Individual channels for SJ protein staining are shown in (B'-H'). Note that Mcr, Cont, Nrx-IV,
754 and Cora become enriched at the apical-lateral region of FCs membrane (arrow in B, D, F, and
755 H). The expression of all of these proteins persists in stage 14 egg chambers (C, E, G, and I).
756 Anterior is to the left. Scale bar = 25µm in B, D, F, and H and 100µm in C, E, G, and I.
757
758 **Figure 3. Mcr, Cont, Nrx-IV, and Cora expression in the germarium.** (A) Diagram of a
759 germarium showing regions 1 and 2 (the full germarium has 3 regions). Terminal filament (TF)
760 and cap cells (CPCs) reside at the most anterior tip of the germarium. In region 1, germline stem
761 cells (GSCs) divide to give rise to a cystoblast (CB), which undergoes four rounds of cell
762 division forming a 16-cell cyst (CCs). In region 2a of the germarium, CCs move posteriorly as
763 they are encapsulated by the prefollicle cells in region 2b. (B-E) Confocal optical sections of
764 wild type germaria stained with antibodies against Mcr (B and single channel in B'), Cont (C and
765 C'), Nrx-IV (D and D'), and Cora (E and E') and co-stained with antibodies against Sxl (B) or

766 Ecad (green) and labeled with DAPI (blue) (C-E). (B) Mcr is highly expressed in GSCs
767 (asterisks), CBs (arrow), and developing cysts (arrowhead), whereas Cont is found in puncta
768 throughout the germarium region (C). Nrx-IV is found in puncta throughout the germarium and
769 outlines the TFs (arrow in D) and the outside membrane of region 1 and region 2a (arrowheads
770 in D). However, the localization of Nrx-IV at the outside membrane in the germarium varies as it
771 was observed in 5 out of 7 germaria examined. (E) Cora is expressed throughout the germarium
772 with high level in the TF (arrow), CPCs (arrowhead) and ESCs (yellow arrows). Anterior is to
773 the left. Scale bar= 25µm.
774
775 **Figure 4. *SJ* genes are required for egg elongation.** (A-G) Brightfield photomicrographs of
776 stage 14 egg chambers. (A) *GR1-GAL4>UAS-GFP*, (B) *GR1-GAL4>UAS-Cont-RNAi*, (C) *GR1-*
777 *GAL4>UAS-Nrx-IV-RNAi*, (D) *GR1-GAL4>UAS-Mcr-RNAi*, (E) *GR1-GAL4>UAS-Cora-RNAi*,
778 (F) *GR1-GAL4>UAS-Sinu-RNAi*, and (G) *GR1-GAL4>UAS-Lac-RNAi*. Images in this figure
779 represent average phenotypes observed in each genotype. (H and I) Quantification of length and
780 width of stage 14 egg chambers from control and *SJ-RNAi* egg chambers. (J) Quantification of
781 the aspect ratio of length (orange line in A) to width (yellow line in A) from control and *SJ-RNAi*
782 stage 14 egg chambers. Note that the aspect ratio of all *SJ-RNAi* expressing egg chambers are
783 statistically significant from the control egg chambers (unpaired T-test; $P<0.0001$). (K) Zoom in
784 images of *GR1-GAL4>UAS-GFP* and *GR1-GAL4>UAS-Lac-RNAi* stage 14 egg chambers
785 showing the dorsal appendages (L). In the control, dorsal appendages are formed, whereas the
786 dorsal appendages in eggs expressing *Lac-RNAi* are either deformed or absent (arrows). (M)
787 Quantification of dorsal appendage defects from control and *SJ-RNAi* stage 14 egg chambers. *n*,

788 total number of egg chambers measured per genotype. Data represents individual values with
789 mean ± s.d. *P* value <0.0001. Anterior is to the left. Scale bar = 100μm.
790
791 **Figure 5. Mcr expression during border cell migration.** (A) Diagram of border cell migration.
792 At early stage 9 of oogenesis, a group of 4-6 follicle cells are specified by the polar cells (PCs)
793 (yellow) to become border cells (BCs) (red). The BC/PC cluster delaminates apically and
794 migrates between the nurse cells (NCs) until it reaches the oocyte (Oo.) by stage 10 of oogenesis.
795 (B-D) Confocal optical images of wild type stage 9-10 egg chambers (insets show border cell
796 clusters) stained with antibodies against Mcr (red and in ” channel), Fas3 (green and in ”’
797 channel), and labeled with DAPI (blue and in ”” channel). Mcr is expressed in the PCs and BCs
798 with the highest expression at the interface between the PCs and BCs. Mcr is also enriched at the
799 leading edge of migration (red arrows in B”-D”). Anterior is to the left. Scale bar = 25μm in (B-
800 D) and 10μm in (B’-B’’’’ through D’-D’’’’).
801
802 **Figure 6. Mcr, Cont, Nrx-IV, and Cora are required for effective border cell migration.** (A-
803 C) Border cell migration in control egg chambers. Confocal optical section of *Slbo>mCD8-GFP*
804 egg chambers immunostained with anti-Fas3 (red) to mark the polar cells, GFP (green) to mark
805 border cells and labeled with DAPI (blue). Arrow indicates a border cell cluster that has
806 completed migration to the oocyte by stage 10. (D-F) Stage 10 egg chambers expressing *Cont-*
807 *RNAi* in border cells immunostained with anti-Cont (red) and anti-Fas3 (blue) as examples of BC
808 cluster migration defects in *SJ-RNAi* egg chambers. Failed (arrow in D), incomplete (arrow in E;
809 note two dashed lines indicate the range of distance at which border cell cluster was categorized
810 as incomplete), or disassociated border cell migration (arrow in F). Higher magnification of wild

811 type (G) and Cont-RNAi-expressing (H) border cell cluster showing the dissociation of border
812 cell cluster observed in *SJ-RNAi* clusters. (I and J) Quantification of border cell cluster
813 phenotypes at stage 10 egg chambers in control and *SJ-RNAi* driven by either Slbo-GAL4 (I) or
814 C306-GAL4 (J) line. Anterior is to the left. Scale bar = 25μm.
815
816 **Figure 7. SJ localization of Cora and Mcr depends on the expression of other SJ proteins.**
817 (A-D) Confocal optical sections of stage 12 follicle cells (FCs) stained with Mcr (red and ’
818 channel) and Cora (green and ” channel) and labeled with DAPI (blue). In wild type FCs, Mcr
819 and Cora co-localize in the region of the SJ (A), whereas Mcr and Cora are mislocalized along
820 the lateral membrane of *NrxIV-RNAi* expressing FCs (B). In *Mcr-RNAi* expressing FCs, Cora is
821 mislocalized laterally (C), however, when Cora appears to maintain its enrichment at the SJ, we
822 often see residual Mcr protein (arrow, D). Scale bar = 10µm (A-D) and 0.5µm (E and F).
823
824 **Figure 8. SJ localization of Cora and Mcr requires Rab5 and Rab11.** (A and B) Confocal
825 optical sections of stage 10 follicle cells (FCs) expressing Rab5-YFP (A) or Rab11-YFP (B)
826 stained with antibody against GFP (green and ’ channel) and Mcr (red and ” channel). Mcr
827 cytoplasmic puncta partially co-localize with Rab5 (white circles) (A-A’’) and Rab11 (B-B’’).
828 (C and D) Confocal optical sections of stage 11 control (C) and Rab5^{DN} expressing (D) FCs
829 expressing Mcr (red and in ’ channel) and Cora (green and in ” channel) and labeled with DAPI
830 (blue). Note that Mcr and Cora co-localize at the region of the SJ in control FCs (arrows), but are
831 mislocalized along the lateral membrane in Rab5^{DN} FCs. (E and F) Confocal optical sections of
832 stage 12 control (E) and Rab11-RNAi expressing (F) FCs expressing Mcr (red and in ’ channel)
833 and Cora (green and in ” channel) and labeled with DAPI (blue). Mcr and Cora are mislocalized

834 in Rab11-RNAi expressing FCs (compare arrows in E and F). In some instances, it appears that
835 Mcr is lost from the membrane in Rab11-RNAi expressing FCs (arrowhead in F). Anterior is to
836 the left. Scale bars = 10µm.
837
838

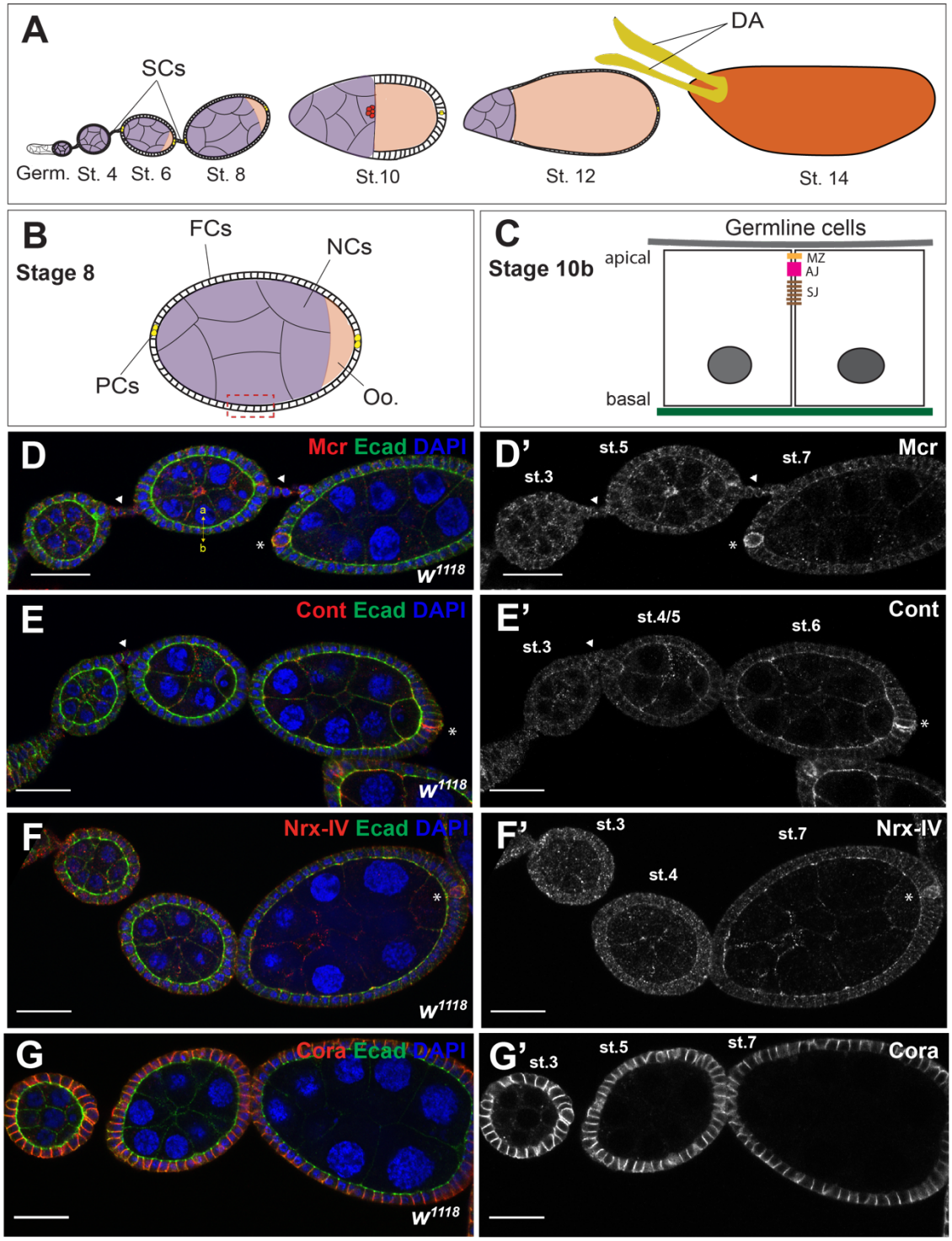
A
SCs
DA
Germ.
St. 4
St. 6
St. 8
St.10
St. 12
St. 14
B
Stage 8
FCs
NCs
PCs
Oo.
C
Stage 10b
Germline cells
apical
basal
MZ
AJ
SJ
D
Mcr Ecad DAPI
w1118
D'
st.3
st.5
st.7
Mcr
E
Cont Ecad DAPI
w1118
E'
st.3
st.4/5
st.6
Cont
F
Nrx-IV Ecad DAPI
w1118
F'
st.3
st.4
st.7
Nrx-IV
G
Cora Ecad DAPI
w1118
G'
st.3
st.5
st.7
Cora

Figure 1.

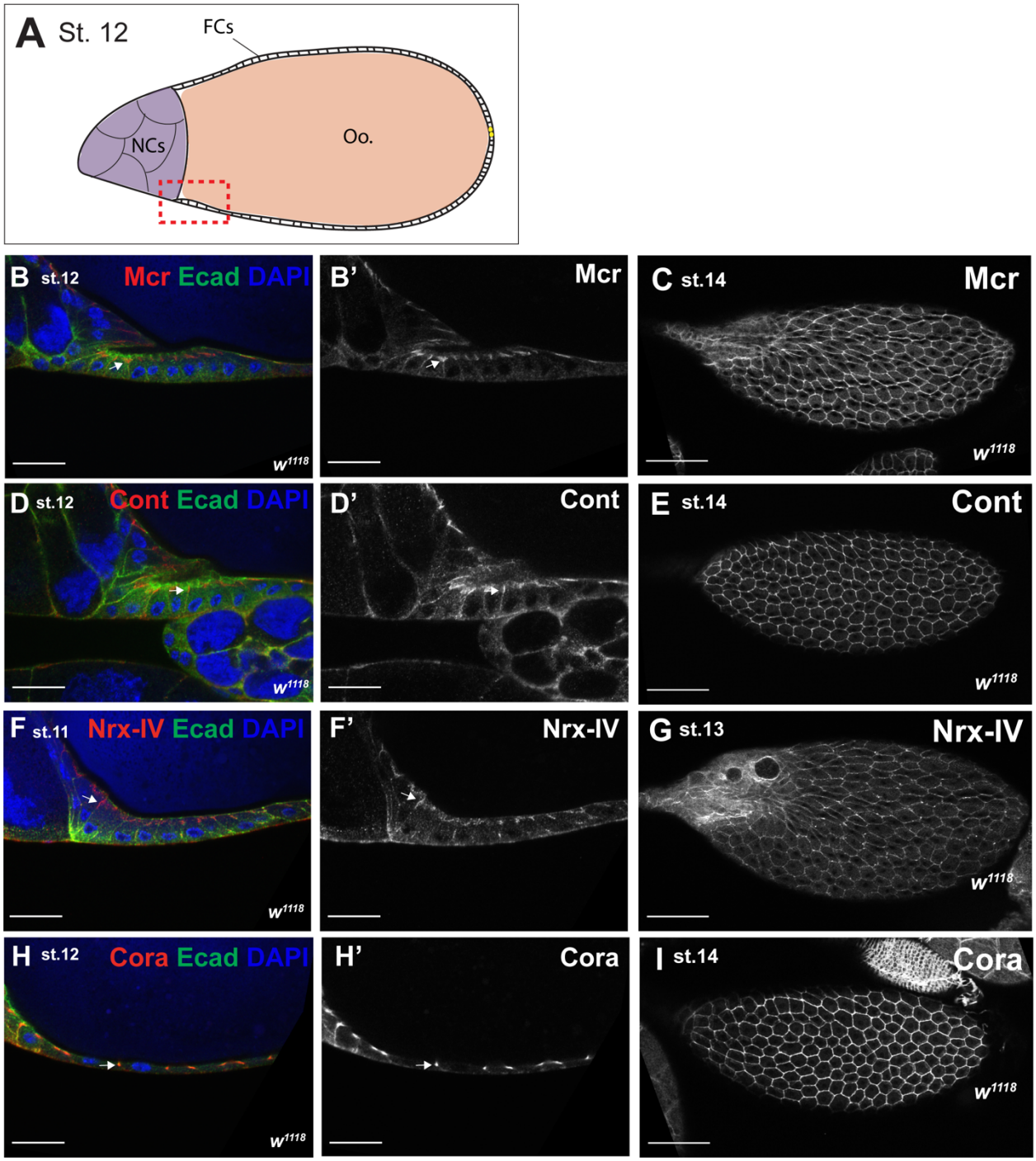
A St. 12
FCs
NCs
Oo.
B st.12
Mcr Ecad DAPI
w1118
B'
Mcr
C st.14
Mcr
w1118
D st.12
Cont Ecad DAPI
w1118
D'
Cont
E st.14
Cont
w1118
F st.11
Nrx-IV Ecad DAPI
w1118
F'
Nrx-IV
G st.13
Nrx-IV
w1118
H st.12
Cora Ecad DAPI
w1118
H'
Cora
I st.14
Cora
w1118

Figure 2.

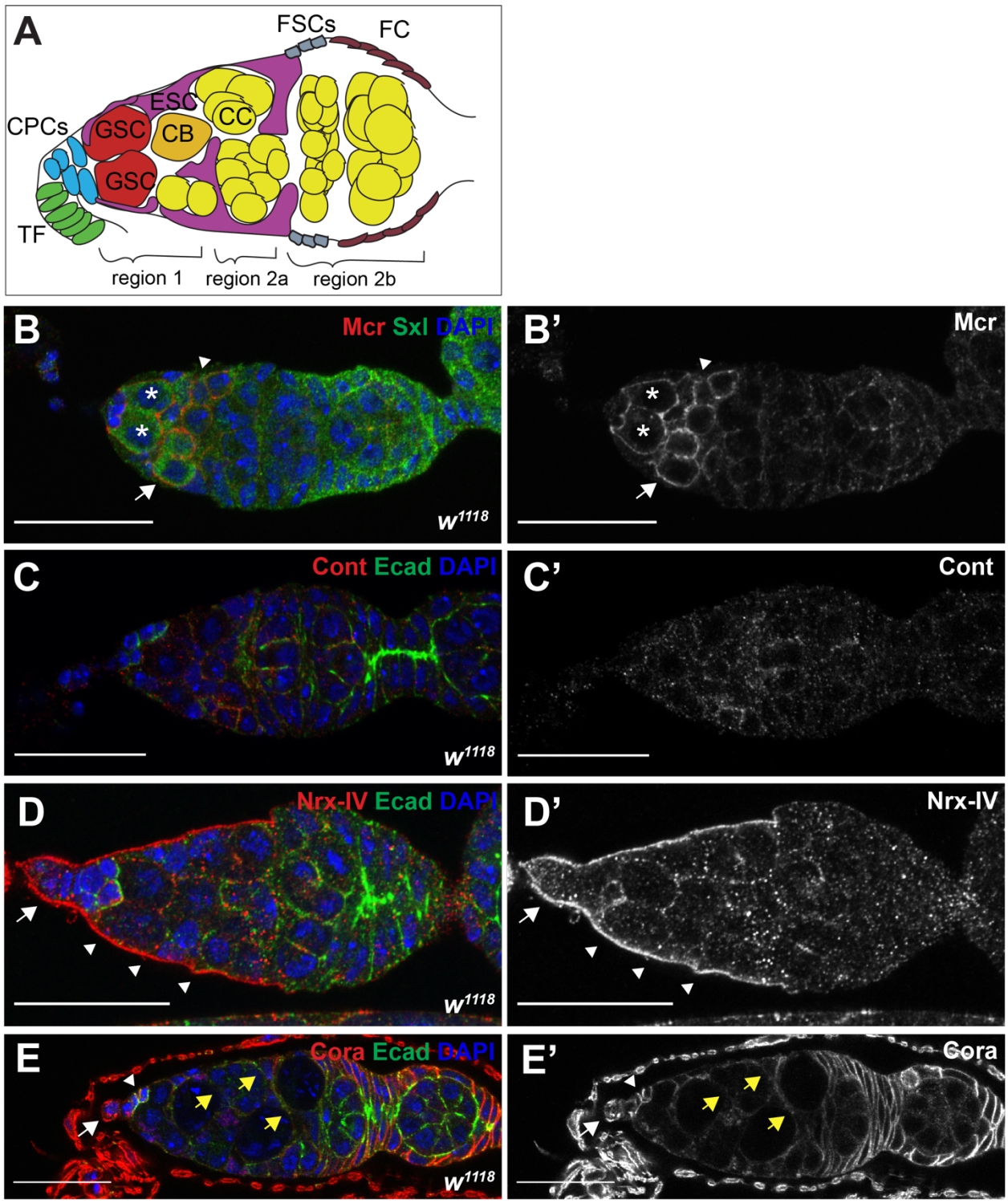
A
FSCs
FC
ESC
CC
CPCs
GSC
CB
GSC
TF
region 1
region 2a
region 2b
B
Mcr Sxl DAPI
w1118
B'
Mcr
C
Cont Ecad DAPI
w1118
C'
Cont
D
Nrx-IV Ecad DAPI
w1118
D'
Nrx-IV
E
Cora Ecad DAPI
w1118
E'
Cora

Figure 3.

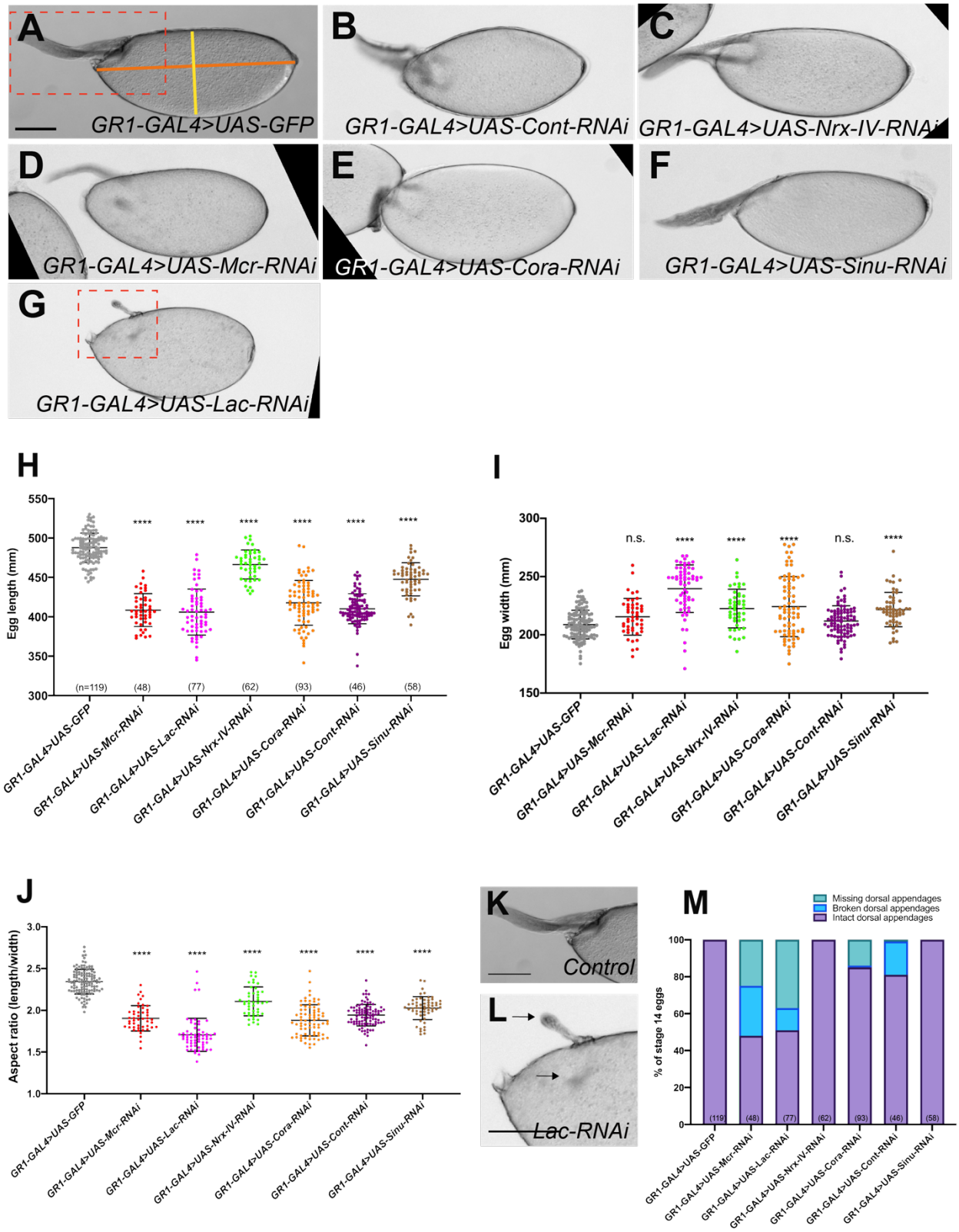
A
GR1-GAL4>UAS-GFP
B
GR1-GAL4>UAS-Cont-RNAi
C
GR1-GAL4>UAS-Nrx-IV-RNAi
D
GR1-GAL4>UAS-Mcr-RNAi
E
GR1-GAL4>UAS-Cora-RNAi
F
GR1-GAL4>UAS-Sinu-RNAi
G
GR1-GAL4>UAS-Lac-RNAi
H
Egg length (mm)
550
500
450
400
350
300
****
(n=119)
(48)
(77)
(62)
(93)
(46)
(58)
GR1-GAL4>UAS-GFP
GR1-GAL4>UAS-Mcr-RNAi
GR1-GAL4>UAS-Lac-RNAi
GR1-GAL4>UAS-Nrx-IV-RNAi
GR1-GAL4>UAS-Cora-RNAi
GR1-GAL4>UAS-Cont-RNAi
GR1-GAL4>UAS-Sinu-RNAi
I
Egg width (mm)
300
250
200
150
n.s.
****
n.s.
J
Aspect ratio (length/width)
3.0
2.5
2.0
1.5
1.0
K
Control
L
Lac-RNAi
M
Missing dorsal appendages
Broken dorsal appendages
Intact dorsal appendages
% of stage 14 eggs
100
80
60
40
20
0

Figure 4.

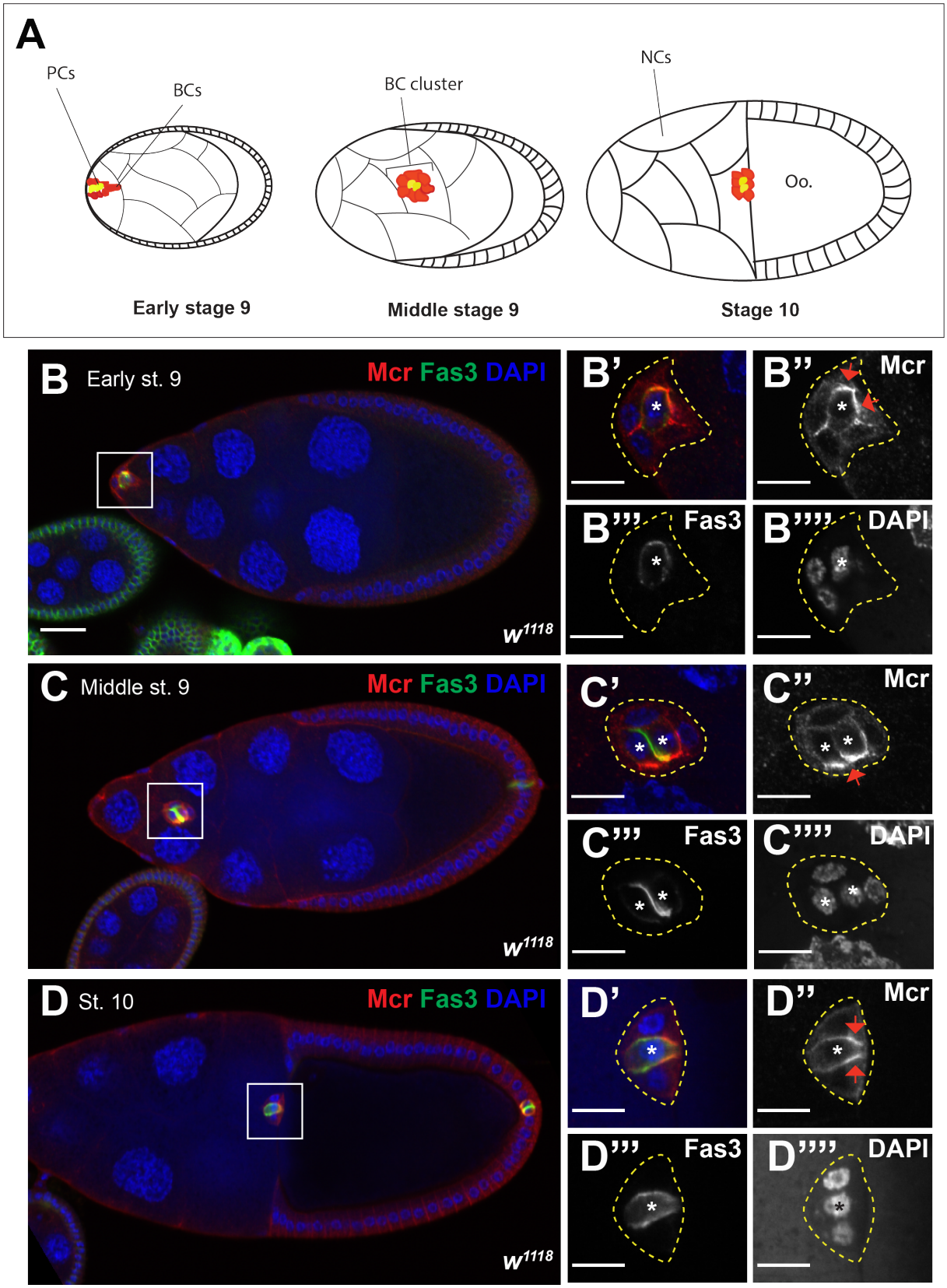
A
PCs
BCs
BC cluster
NCs
Oo.
Early stage 9
Middle stage 9
Stage 10
B Early st. 9
Mcr Fas3 DAPI
w1118
B'
B''
Mcr
B'''
Fas3
B''''
DAPI
C Middle st. 9
Mcr Fas3 DAPI
w1118
C'
C''
Mcr
C'''
Fas3
C''''
DAPI
D St. 10
Mcr Fas3 DAPI
w1118
D'
D''
Mcr
D'''
Fas3
D''''
DAPI

Figure 5.

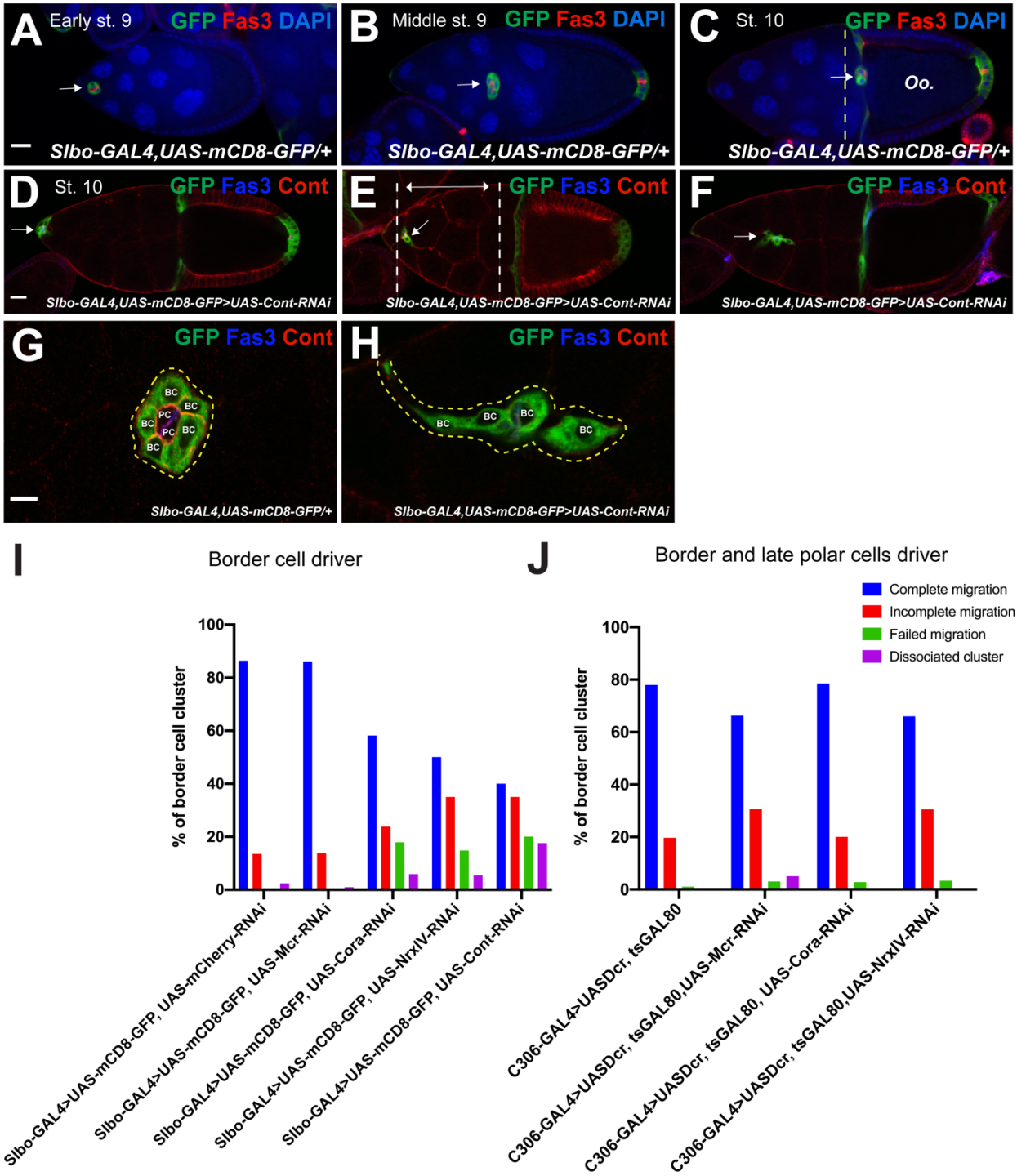
A
Early st. 9
GFP Fas3 DAPI
Slbo-GAL4,UAS-mCD8-GFP/+
B
Middle st. 9
GFP Fas3 DAPI
Slbo-GAL4,UAS-mCD8-GFP/+
C
St. 10
GFP Fas3 DAPI
Oo.
Slbo-GAL4,UAS-mCD8-GFP/+
D
St. 10
GFP Fas3 Cont
Slbo-GAL4,UAS-mCD8-GFP>UAS-Cont-RNAi
E
GFP Fas3 Cont
Slbo-GAL4,UAS-mCD8-GFP>UAS-Cont-RNAi
F
GFP Fas3 Cont
Slbo-GAL4,UAS-mCD8-GFP>UAS-Cont-RNAi
G
GFP Fas3 Cont
BC
PC
Slbo-GAL4,UAS-mCD8-GFP/+
H
GFP Fas3 Cont
BC
Slbo-GAL4,UAS-mCD8-GFP>UAS-Cont-RNAi
I
Border cell driver
% of border cell cluster
0
20
40
60
80
100
Slbo-GAL4>UAS-mCD8-GFP, UAS-mCherry-RNAi
Slbo-GAL4>UAS-mCD8-GFP, UAS-Mcr-RNAi
Slbo-GAL4>UAS-mCD8-GFP, UAS-Cora-RNAi
Slbo-GAL4>UAS-mCD8-GFP, UAS-NrxIV-RNAi
Slbo-GAL4>UAS-mCD8-GFP, UAS-Cont-RNAi
J
Border and late polar cells driver
Complete migration
Incomplete migration
Failed migration
Dissociated cluster
% of border cell cluster
0
20
40
60
80
100
C306-GAL4>UASDcr, tsGAL80
C306-GAL4>UASDcr, tsGAL80,UAS-Mcr-RNAi
C306-GAL4>UASDcr, tsGAL80, UAS-Cora-RNAi
C306-GAL4>UASDcr, tsGAL80,UAS-NrxIV-RNAi

Figure 6.

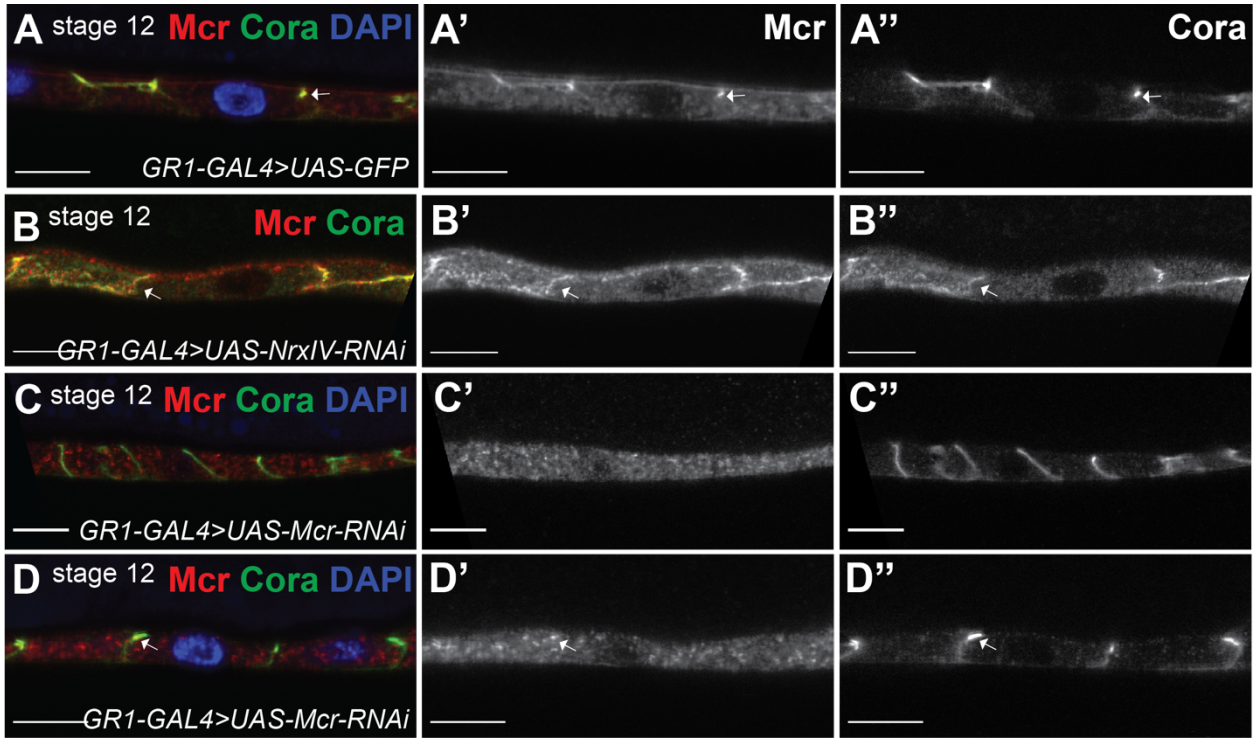
A stage 12 Mcr Cora DAPI
GR1-GAL4>UAS-GFP
A' Mcr
A'' Cora
B stage 12 Mcr Cora
GR1-GAL4>UAS-NrxIV-RNAi
B'
B''
C stage 12 Mcr Cora DAPI
GR1-GAL4>UAS-Mcr-RNAi
C'
C''
D stage 12 Mcr Cora DAPI
GR1-GAL4>UAS-Mcr-RNAi
D'
D''

Figure 7.

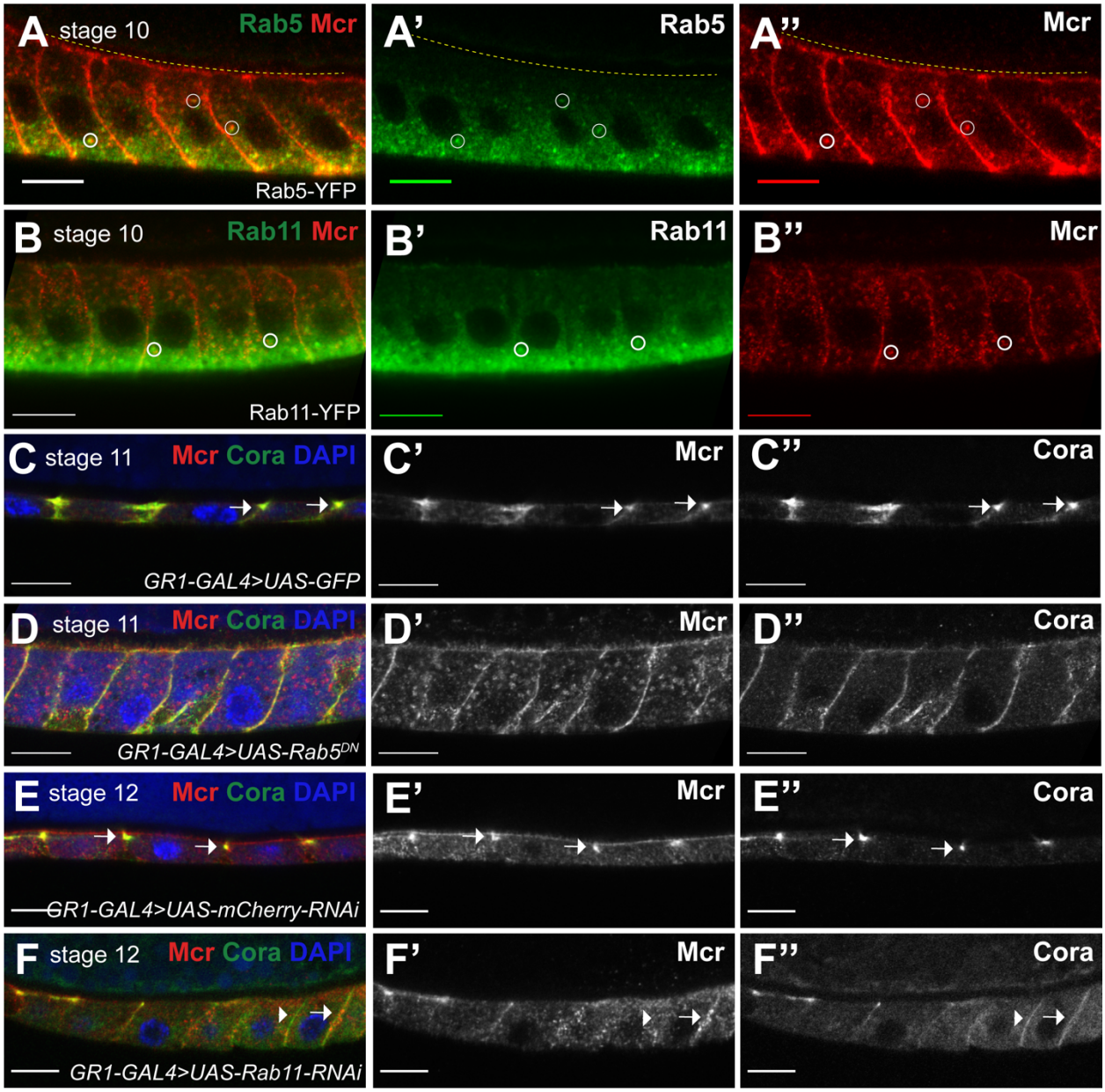
A stage 10
Rab5 Mcr
Rab5-YFP
A'
Rab5
A''
Mcr
B stage 10
Rab11 Mcr
Rab11-YFP
B'
Rab11
B''
Mcr
C stage 11
Mcr Cora DAPI
GR1-GAL4>UAS-GFP
C'
Mcr
C''
Cora
D stage 11
Mcr Cora DAPI
GR1-GAL4>UAS-Rab5DN
D'
Mcr
D''
Cora
E stage 12
Mcr Cora DAPI
GR1-GAL4>UAS-mCherry-RNAi
E'
Mcr
E''
Cora
F stage 12
Mcr Cora DAPI
GR1-GAL4>UAS-Rab11-RNAi
F'
Mcr
F''
Cora

Figure 8.

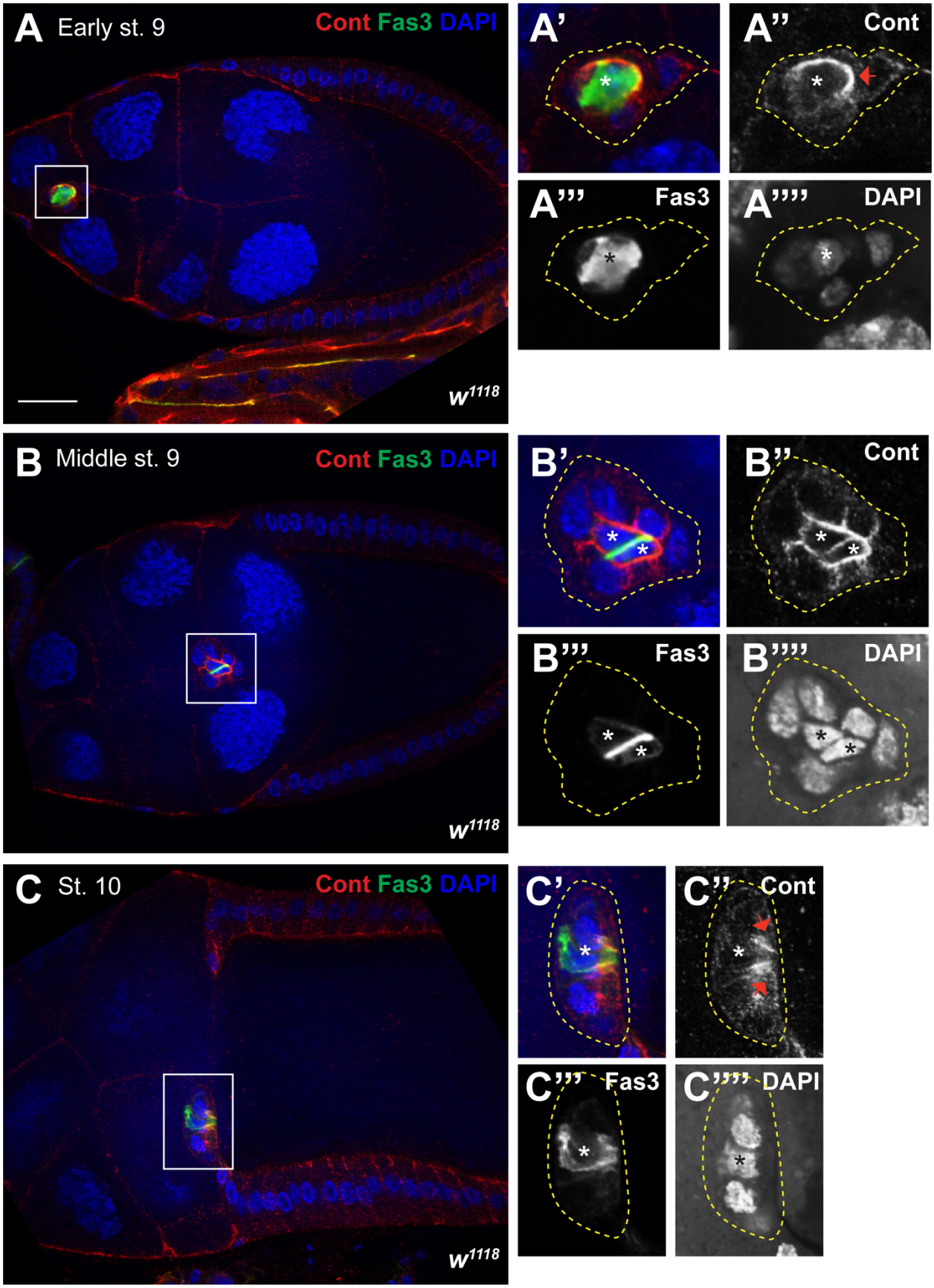
A Early st. 9
Cont Fas3 DAPI
w1118
A'
A''
Cont
A'''
Fas3
A''''
DAPI
B Middle st. 9
Cont Fas3 DAPI
w1118
B'
B''
Cont
B'''
Fas3
B''''
DAPI
C St. 10
Cont Fas3 DAPI
w1118
C'
C''
Cont
C'''
Fas3
C''''
DAPI

Figure S1. Cont expression during border cell migration. (A-C) Confocal optical images of wild type stage 9-10 egg chambers (insets show border cell clusters) stained with antibodies against Cont (red and in ” channel), Fas3 (green and in ”’ channel), and labeled with DAPI (blue and in ”” channel). Cont is expressed in the border cell cluster throughout oogenesis, with high level at the polar cells-border cells interfaces (asterisks in A’, B’ and C’). Anterior is to the left. Scale bar = 25µm.

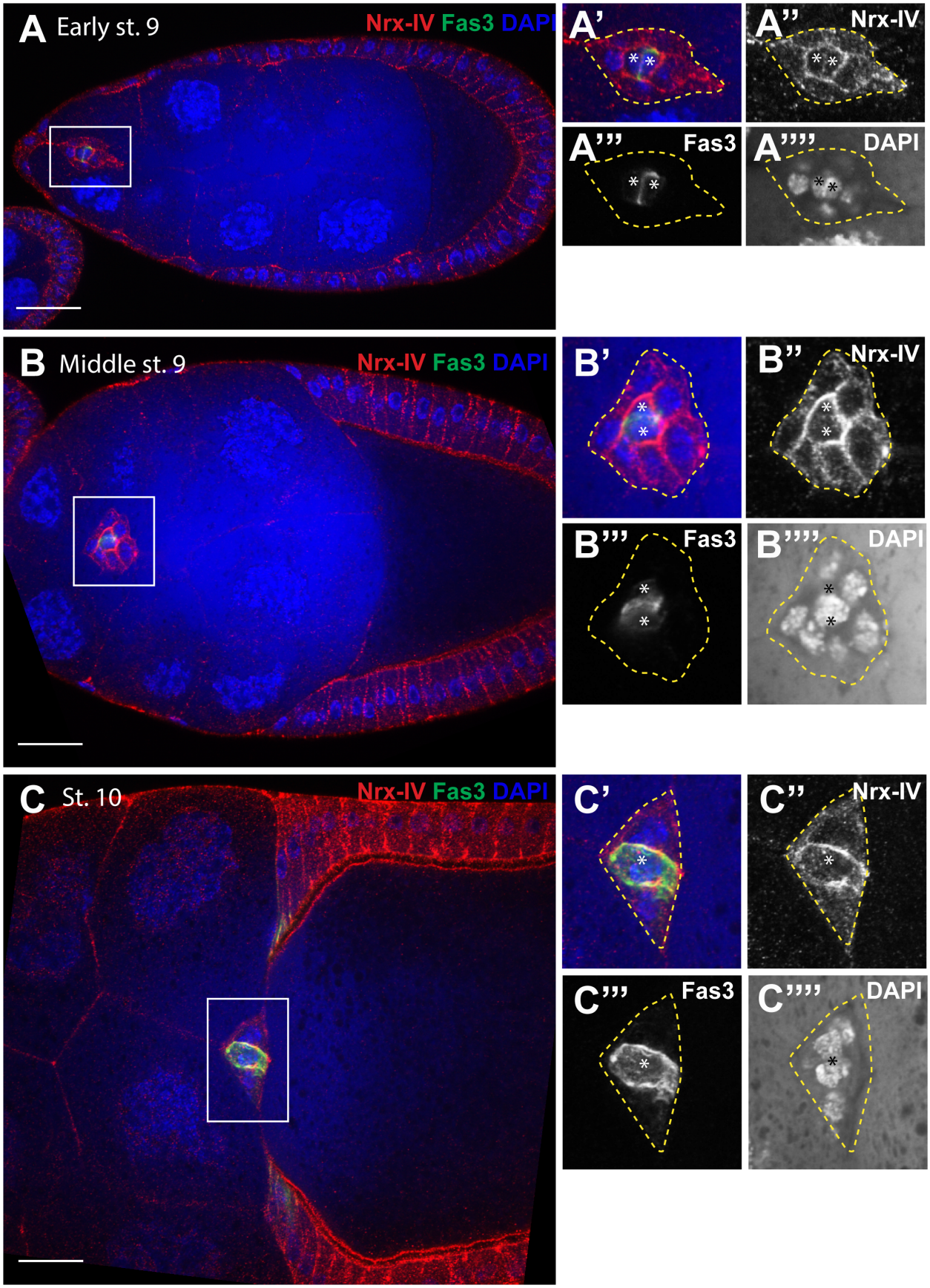
A Early st. 9
Nrx-IV Fas3 DAPI
A'
A''
Nrx-IV
A'''
Fas3
A''''
DAPI
B Middle st. 9
Nrx-IV Fas3 DAPI
B'
B''
Nrx-IV
B'''
Fas3
B''''
DAPI
C St. 10
Nrx-IV Fas3 DAPI
C'
C''
Nrx-IV
C'''
Fas3
C''''
DAPI

Figure S2. Nrx-IV expression during border cell migration. (A-C) Confocal optical images of wild type stage 9-10 egg chambers (insets show border cell clusters) stained with antibodies against Nrx-IV (red and in ” channel), Fas3 (green and in ”’ channel), and labeled with DAPI (blue and in ”” channel). Nrx-IV is expressed in both polar cells (PCs) and border cells (BCs) throughout border cell migration, with high level at the PCs-BCs interfaces (asterisks in A’, B’ and C’). Anterior is to the left. Scale bar = 25µm.

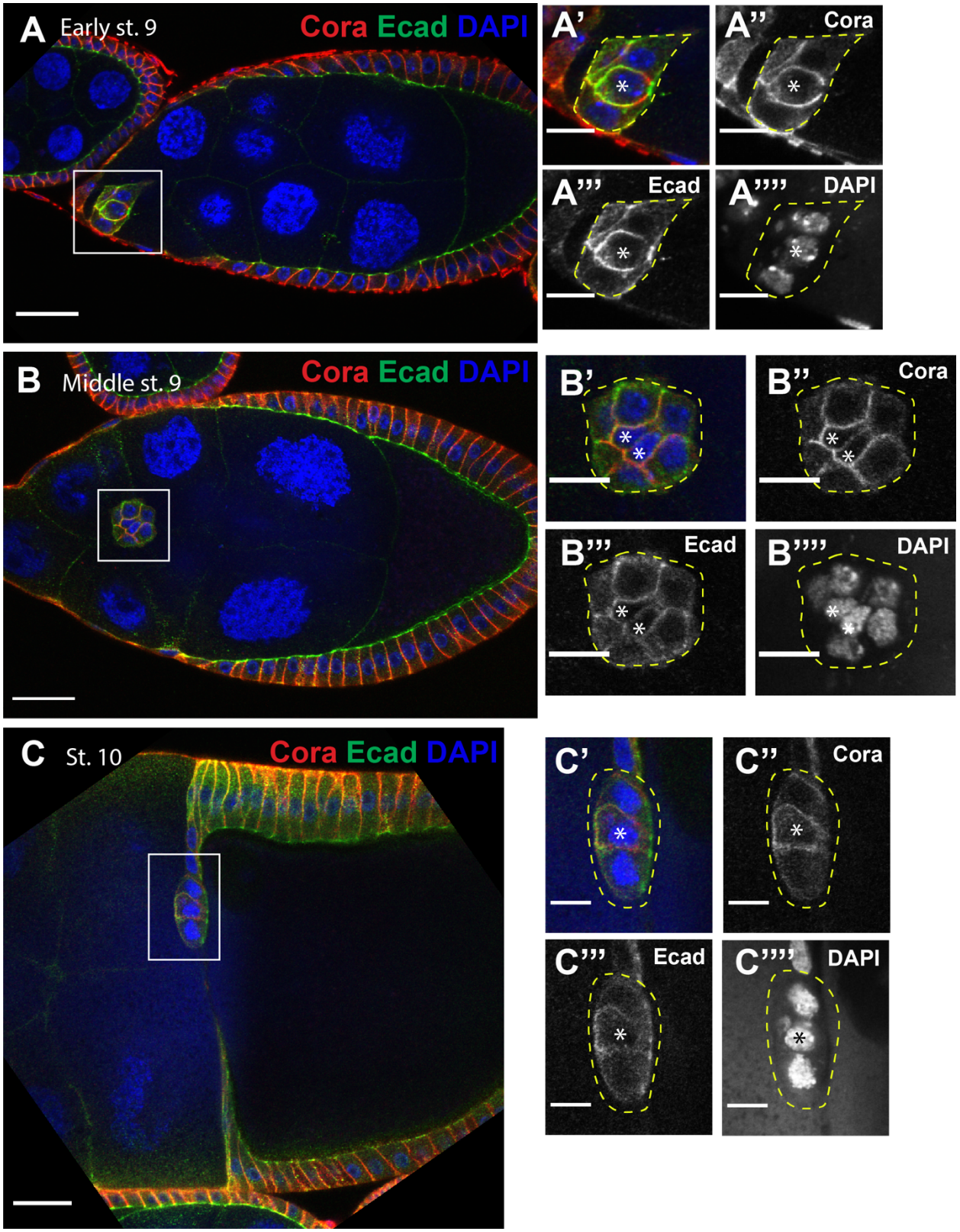
A Early st. 9
Cora Ecad DAPI
A'
A''
Cora
A'''
Ecad
A''''
DAPI
B Middle st. 9
Cora Ecad DAPI
B'
B''
Cora
B'''
Ecad
B''''
DAPI
C St. 10
Cora Ecad DAPI
C'
C''
Cora
C'''
Ecad
C''''
DAPI

Figure S3. Cora expression during border cell migration. (A-C) Confocal optical images of wild type stage 9-10 egg chambers (insets show border cell clusters) stained with antibodies against Cora (red and in ” channel), Fas3 (green and in ”’ channel), and labeled with DAPI (blue and in ”” channel). (A) At early stage 9, Cora is expressed in both polar cells (PCs) and border cells (BCs). (B) During middle stage 9 of oogenesis, Cora continues to be expressed in the cluster until stage 10 with the highest level in the PCs relative to the BCs (C) (asterisks in A’, B’ and C’). Anterior is to the left. Scale bar in A-C = 25µm and 10µm in A’-A’’’’, B’-B’’’’, and C’-C’’’’.